



The University of
Nottingham

2024

UNITED KINGDOM • CHINA • MALAYSIA

**Preliminary System Design for the Development of
CubeSat with GNSS-Reflectometry (GNSS-R)
Payload for Monitoring Sea Level Change**

Name: Helen Haile

Student Number: 20612508

**Submitted in partial fulfilment of the requirements for the Degree
of MRes Geospatial Data Science,**

Faculty of Engineering, University of Nottingham.

Nottingham Geospatial Institute

School of Engineering Surveying and Space Geodesy

30 Triumph Road,

Nottingham NG7 2TU

United Kingdom.

Date: 15/09/2024

HELEN HAILE

ABSTRACT

Global warming is causing a rapid rise in sea levels. This is particularly pressing as the impacts are causing flooding, salinisation, extreme weather and sea temperature, and threatening food security. The impacts are particularly severe for communities in the global south and developing countries due to significant social and economic injustice. With approximately 600 million people living in coastal regions globally, the potential submerges in this area could lead to further economic impact and increase the social and economic effects felt in the global south and coast area.

This project aims to assess the feasibility of cost-effective, compact, and capable CubeSats in Low Earth Orbit (LEO) that can measure levels daily. This approach will enhance our understanding and monitor sea level change. Over the past 30 years, satellite missions have contributed significantly to sea level rise altimetry, providing long-term observational records and offering a better understanding of sea level changes across oceans and seas. However, traditional Ocean altimetry relies on large, costly satellites designed primarily for open ocean research and struggles to capture altimetry in coastal regions with the necessary spatial and shorter temporal scales.

To address this gap in consistent, reliable altimetry in coastal areas, the CubeSats will utilise GNSS-Reflectometry (GNSS-R). GNSS-R is an innovative remote sensing technique with a higher temporal and spatial resolution than traditional radar altimetry.

The mission will deploy eight CubeSat 6u on a single orbital plane, with a spacing of 45° between them. All the satellites will be placed in Sun-Synchronous Orbit (SSO) at an altitude of 550km, providing 15 revisit times per day for one satellite revisit time.

The feasibility indicates that GNSS-R provides a promising alternative to traditional innovative remote sensing, offering reduced mass and power requirements. This will offer a cost-effective sea-level measurement approach.

Table of Contents

ABSTRACT.....	1
1. Introduction	4
1.1 Sea-level Rise	4
1.2 Aims and Objectives.....	5
2. Review Of Existing Literature	6
2.1 Overview of Sea Level Monitoring Methods.....	6
2.1.1 Tide Gauges.....	6
2.1.2 Satellites Remote Sensing for Sea Level Change	7
2.1.3 Capabilities and Challenges of Key Sea level Monitoring Missions	12
2.1.4 Applications GNSS Reflectometry for Sea Level Measurement	12
2.1.5 GNSS Reflectometry Missions for Sea Level Measurement.....	15
2.2 GNSS-R Technology for CubeSats	17
2.2.1 CubeSats for Sea Level Monitoring	17
2.3 Evaluation of Current Limitations in Sea Level Monitoring.....	19
3. Methodology.....	20
3.1 Methodology Implementation Process.....	21
3.1.1 Orbital Parameters Requirements.....	21
3.1.2 GNSS-R Payload and Altimeter System Requirement	22
3.1.3 Preliminary System Requirements and System Design.....	22
4. Results	23
4.1 Mission Objectives	23
4.2 Mission Concept.....	23
4.2.1 Orbit Design and Analyses	23
4.2.2 Concept of Operation (In-Orbit Operations).....	24
4.2.3 GNSS-R Payload.....	25
4.2.4 Constellation	26
4.3 Mission Analysis.....	26
4.3.1 Lifetime Analysis	26
4.3.2 Access Time Analysis.....	27
4.4 Satellite Subsystem Design	28
4.4.1 Platform.....	28
4.4.2 Communication	29
4.4.3 Attitude Determination and Control Subsystem and On-Board Computer(OBC).....	30
4.4.4 Electrical Power System (EPS)	31
4.4.5 Mass Budgets	32

5. Discussion.....	33
5.1 Finding.....	33
6. Conclusion.....	34
7. Recommendations for Further Work	34
8. References.....	35
8. Appendices.....	0
Appendix A: Project Plan.....	0
Appendix B: Orbital calculation.....	0
Appendix C: Constellations Calculation	2
Appendix D: Power calculation	4
Appendix E Payload Description	5

1. Introduction

1.1 Sea-level Rise

The impact of climate change has been a global agenda in recent years, and it has captured public, political and scientific interest globally. The key drivers of climate change are greenhouse gases, which have led to higher temperatures and rising sea levels, including precipitation and extreme weather changes. Further, changes have accelerated the melting of polar ice, causing an increased sea level. The rise in sea level is particularly pressing as the impacts are manifested in erosion, flooding, salinisation, extreme weather events cascading effects and as a pattern of tropical and extratropical cyclones, rising air, and sea temperatures (Roy et al. 2023). The most urgent challenge is the rising sea level in coastal regions worldwide, and the impacts are on human settlements, infrastructure, and ecosystems near the coast. The impacts are particularly felt around the coastal area in those counties, depending on the coastal economic, social, and environmental benefits. According to (Fasullo et al. 2020), coastal regions globally accommodate about 600 million people; the numbers will double by 2060. The coastal communities are most susceptible to sea level rise as the impact can cause coastal erosion, limiting their land area and forcing them to relocate to dry areas (See Table 1 and Figure 1). (Adebisi, A.-L. Balogun, et al. 2021) report that since the recording of the sea level began in 1880, the Global Mean Sea level has risen by about 16–21 cm, with more than 7 cm of this occurring since 1993. M.S. Swaminathan Research Foundation predicts a rise of between 16 cm and 32 cm by the years 2050 and 2100.

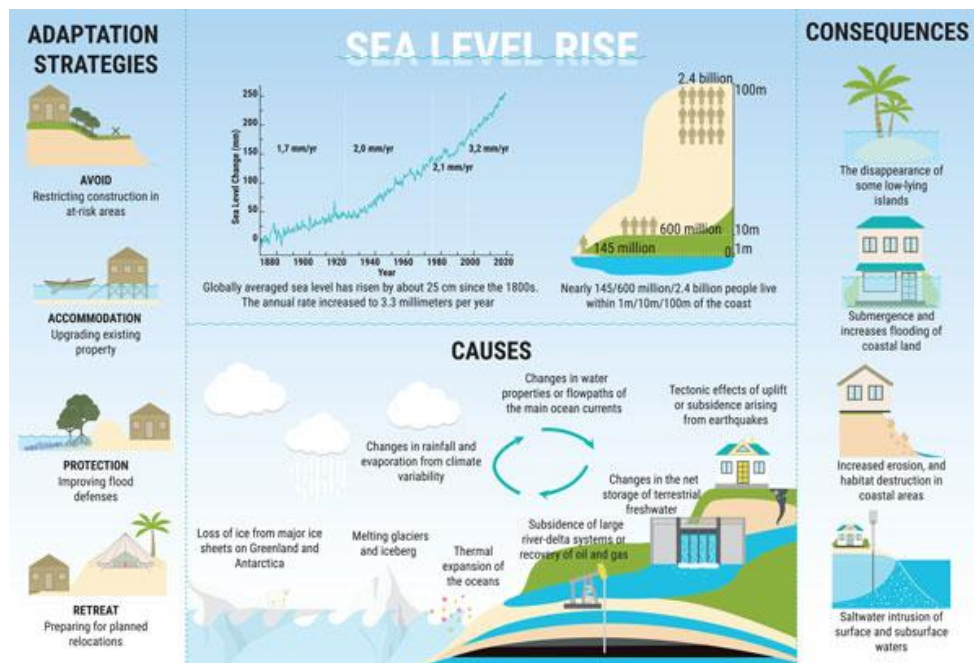


Figure 1 Sea Level Rise (youmatter.world, 2019)

Tourism contributes about 11% of Spain's Catalan region's gross domestic product (GDP). (Garola et al. 2022) conducted an economic impact analysis of sea level-induced erosion on Catalan beaches. The impact expected on GDP loss is approximately 2200 million € and 1820 million € (at 2019 values), respectively. For instance, (Davis Dexter et al. 2010) highlight that many Caribbean populations live and work in coastal regions, with significant infrastructure such as international airports, roads, and capital cities located there. A 1-meter sea level rise could submerge 98 coastal communities,

threatening approximately 50,000 people and the entire island. This would result in substantial economic impact, including job loss and distributions in the coastal economy and effects on other productive sectors such as public services and administration.

The coastal zone is dynamic, influenced by winds and ocean circulation, which distribute heat content and mass changes around the oceans (See Table 1). This variability creates complex regional and different variations of sea level regional sea levels; therefore, this has increased the demand for regional sea level estimates (Hamid et al. 2018).

Table 1 The Impacts of Extreme Coastal Water Level

Impact	Main contributors
Destruction of shoreline defences	Waves, swell, surge
Coastal erosion	Waves, swell, surge
Altered estuarine dynamics and morpho-dynamics	Tides
High tide flooding	Tides
Catastrophic flooding	Any factors combined

Therefore, understanding Sea level rise trends and accurately measuring sea levels is crucial for effective adaptation and mitigation strategies. These insights enable policy and decision-makers to make evidence-based decisions to implement effective mitigation and measures. The impact of rising sea levels requires frequent monitoring to evaluate its effect on coastal residents. This research also indicates the potential for positive climate change monitoring and coastal management changes through freely available GNSS signals.

1.2 Aims and Objectives

This work aims to assess the feasibility of deploying a constellation of CubeSats in Low Earth Orbit (LEO) to obtain daily measurements of sea levels in coastal areas. The study will evaluate the limitations of the current radar altimetry methods and explore whether innovative and cost-effective approaches, such as GNSS-Reflectometry (GNSS-R), can enhance sea level measurement in coastal regions.

Using the European Cooperation for Space Standardization ECSS-(ECSS--M--30--01A) design methodologies. This study will focus on Phases 0 and A ECSS standards to achieve the following objectives.

1. Mission objective: analysis of top-level mission requirements and design mission success criteria for sea level monitoring
2. Mission concept: Determining optimal orbit design, developing the operation concept, and conducting constellation analyses to ensure and enhance coverage in coastal regions.
3. Mission analyses: Perform access time and lifetime analysis to evaluate the operational
4. Satellite subsystem analysis: assess the CubeSat subsystem, calculate the data rate required to meet the mission objective and analyse the mass and power budget for the mission

The outcome of this study will contribute to the future preliminary design of the CubeSat mission and constellation design.

2. Review Of Existing Literature

2.1 Overview of Sea Level Monitoring Methods

Sea level measurement began around 1880. Continuity in observations over time is crucial for providing real-time temporal data, enabling insight into temporary changes and long-term trends. According to (Hannah 2010), at least 60 years of continuous and accurate sea level data is required to understand past patterns and current trends and estimate future scenarios. The primary monitoring methods for sea level are tide gauges and satellite altimetry. Tide gauges provide detailed long-term data at specific locations with higher resolution closer to coastlines. Over the last 30 years, satellite missions have contributed significantly to sea level rise altimetry, covering global sea level changes at different spatial resolutions and offering a better understanding of sea level changes across oceans and seas with long-term observational records (Gower, Barale 2024).

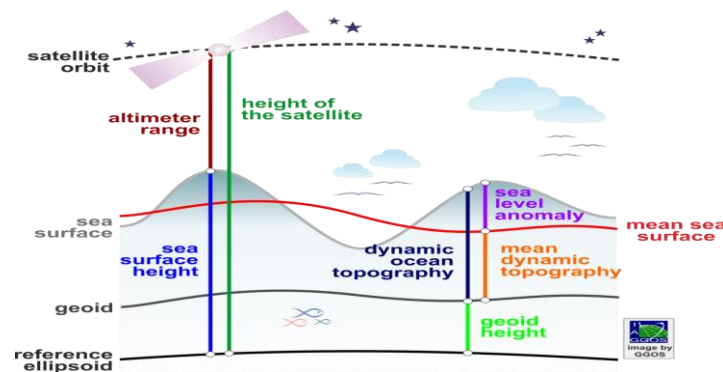


Figure 2 Sea Level Measurement Monitoring Ecosystem (GGOS Global Geodetic Observing System)

2.1.1 Tide Gauges

Tide gauges are the earliest sea level rise (SLR) measurement, operated by documenting the time and height of tidal high and low waters with the tide poles. This method allows for measuring sea level changes at specific locations and relative to the ground on which these gauges are installed, as illustrated in Figures 1 and 2. For the data gathered by tide gauges to remain continuous and stable, it is imperative that these gauges are integrated into the corresponding national geodetic networks (Marcos et al. 2019). Additionally, to accurately disentangle land and ocean contributions to sea-level changes recorded by tide gauges, it is crucial to have precise estimates of long-term vertical land motion. Tide gauges offer detailed insights into long-term sea level changes at the specific installation sites. However, they are not without their limitations.

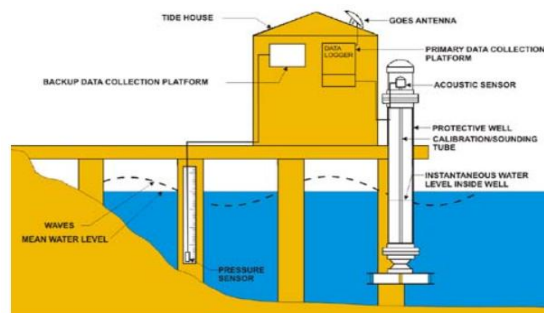


Figure 3 Tidal Monitoring Stations (The National Ocean Service US)

Further, (Adebisi, A. L. Balogun, et al. 2021) explained that one of the main advantages of tide gauges is that they provide detailed long-term sea level change information at a fine temporal scale at the specific locations of installations. However, they often produce inconsistent observational data due to their uneven geographic distribution and the lack of a uniform reference level for all tidal records, as shown in Figure 3. Additionally, their effectiveness is compromised by vertical land movement or seismic activity disruption.

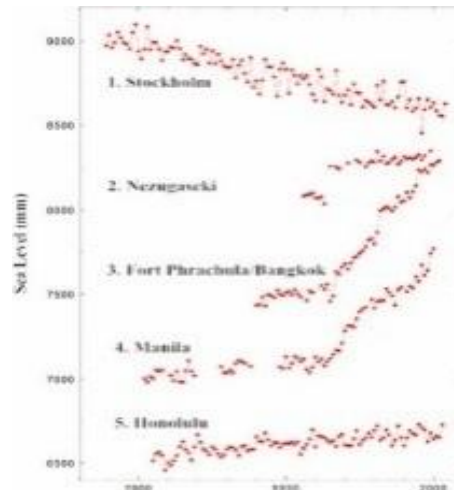


Figure 4 Different Tide Gage Measurement Levels Around the Globe (Abdalla et al. 2021)

The spatial and temporal distribution of tide gauge records varies significantly (Marcos et al. 2019), necessitating accurate and consistent long-term data on vertical land motion to effectively separate land and ocean contributions to recorded sea-level changes. Moreover, the distribution of tide gauge networks exhibits considerable bias, with a concentration in Europe and North America and sparse coverage in other regions, particularly Africa and Asia. This geographic imbalance complicates the estimation of global sea level trends using tide gauge data. Furthermore, recording tidal data with tide poles, necessitating constant observation and calibration of the gauges, is susceptible to human error (Adebisi, A. L. Balogun, et al. 2021).

2.1.2 Satellites Remote Sensing for Sea Level Change

Satellite remote sensing for Sea level measurement, a cornerstone of modern oceanography and climate science studies since 1969, has been instrumental in our continuous observation of sea levels. This advancement has provided crucial data for understanding changes on a global scale. Since 1992, satellite remote sensing missions have offered a continuous 30-year time series that has become indispensable to the long-term record of sea level observations. The TOPEX/Poseidon and Jason satellites have pioneered these efforts (Gower, Barale 2024). The development of altimetry technology, with its multidisciplinary application in geodesy, geophysics, and oceanography, has played a vital role in comprehending climate change and its impacts on a global scale (Bašić, Bašić 2023).

The comprehensive nature of satellite remote sensing, which encompasses critical areas such as sea level, sea state, ice, ice sheets, surface current, and changes in lake and river levels, provides a broad and deep understanding of climate dynamics, fostering a cross-disciplinary approach to Earth observation (Abdalla et al. 2021). The remote sensing process involves using sensors from aircraft,

drones, or satellites to gather information about objects from a distance. There are two main types of sensors: active and passive. The figure illustrates that the remote technique can differ depending on the application.

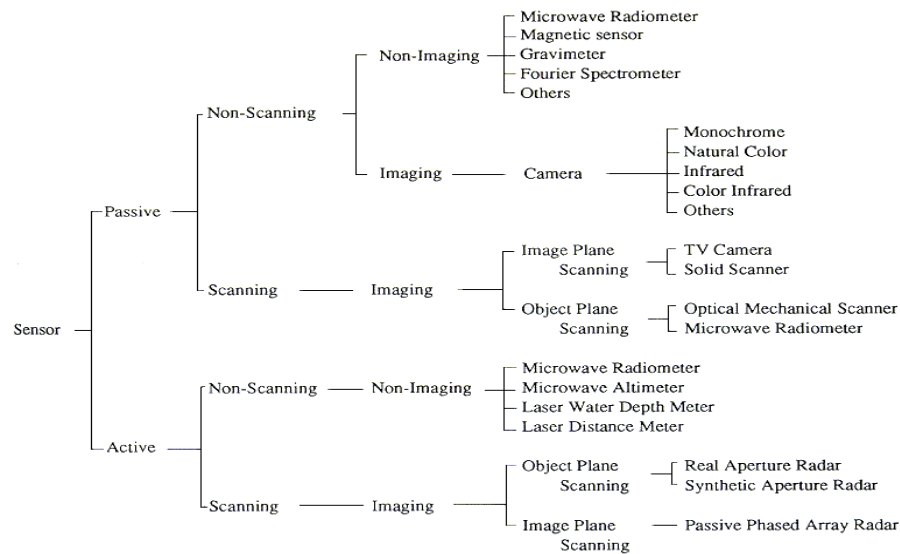


Figure 5 Remote Sensing Sensor Type (Japan Association of Remote Sensing)

Active sensors use pulses or radar technology to measure the two-way travel time between the satellite and the surface to collect data. Passive sensors use multispectral (hyperspectral) sensors to acquire data through band combinations. Measuring sea level rise using active remote sensors has several advantages over passive sensors. Active sensors based on radar technology provide high-precision global sea-level data making them more suitable for sea level measurement. They are less affected by atmospheric conditions, have a higher spatial resolution, and can provide more accurate measurements of sea level changes over time. This makes them a preferred choice for sea level measurement (An et al., 2022) (Bašić, Bašić 2023).

One of the revolutionary aspects of satellite remote sensing is its capacity to monitor sea levels with high spatio-temporal resolution, covering 66° North to 66° South across almost all the ice-free oceans. This enabled measuring sea levels from the top, offering a nearly continuous observation that vastly improved previous methodologies (Marcos et al. 2019). In recent years, the role of remote sensing has become increasingly critical. The technology enables measuring absolute sea level changes over short periods by calculating the distance between the satellite and the planet's surface.

This method addresses the uneven geographical distribution of tide gauges by providing a global perspective, unachievable through other means (Bašić, Bašić 2023). The global average sea level estimation through satellite remote sensing currently stands with an accuracy of 1.67 ± 0.08 cm at a 10-day temporal resolution. Although limited by systematic errors, this precision significantly improves tide gauges. The ability of satellite measurements to tie directly to the Earth's centre of mass, in contrast to tide gauges that are fixed at coastal locations, underscores satellite data's broader applicability and accuracy (Davis Dexter et al. 2010).

The satellite remote sensing measurements process involves transmitting and receiving microwave radar pulses. The onboard radar emits a pulse towards the Earth, and the time taken for the pulse to be reflected and detected by the satellite is used to calculate the sea surface height (SSH); this process is illustrated in Figure 5.

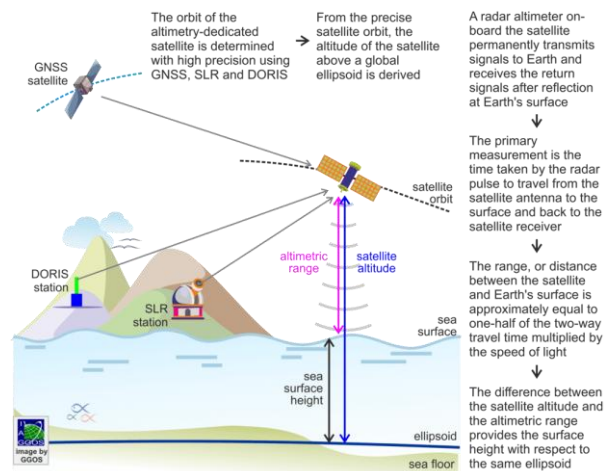


Figure 6 Remote Sensing Satellite Sea level measurement process (GGOS Global Geodetic Observing System)

The correction relationship is expressed in the following equation.

$$Shh = Z - (R + Cor)$$

Cor = atmospheric, geophysical and instrumental corrections.

Once the data are collected, it must be corrected by considering the satellite's altitude and the distance to the sea surface, adjusted for atmospheric and geophysical corrections (Amani et al. 2022a) (L. Sánchez, D. Chambers 2024). The application of sophisticated atmospheric and geophysical models allows for the optimisation of data accuracy, thereby enriching the quality of the information gathered for scientific research and application (Amani et al. 2022a) (L. Sánchez, D. Chambers 2024). In addition, to ensure the accuracy of these measurements, satellites are equipped with advanced tracking systems, such as the Global Navigation Satellite System (GNSS) and the Doppler Orbitography and Radio Positioning Integrated by Satellite (DORIS). Furthermore, adopting nadir or Earth-facing altimetry measurement enhances the reliability of data collection (Ablain et al. 2017).

Table 2 Properties of Radar and Laser Altimeters

Properties	Radar altimeter	Laser altimeter
Footprint	km level	m level
Vertical accuracy	Tens of centimetres	Tens of centimetres
Atmospheric Attenuation	Yes	No
Size and mass	Higher	Lower
Power consumption	Lower	Higher

Many open ocean-monitoring satellites (See Figure 6) use radar altimetry in beam-limited or pulse-limited modes. For the radar signal, the antenna footprint is a crucial factor in satellite altimetry, as it

defines the specific area of the sea surface observed by the altimeter system (Colagrossi et al.,2023). These modes affect the footprint size and, consequently, the accuracy and resolution of the measurements. While the beam-limited mode requires larger antennas for smaller footprints, the pulse-limited mode enables accurate measurements with smaller antennas. The Advancement of missions such as the ERS, Jason, and SARAL/AltiKa utilize pulse-limited altimeters (Cipollini, Snaith 2015) provided an essential tool for observing and understanding the complex dynamics of Earth's oceans.

Satellite / Altimeter	Dates	Radar freq. (GHz)	Band-width (MHz)	Beam-width (°)	Repeat period (days)
ERS-1 / RA	Jul 1991 - Apr 2000	13.8	330	1.3	35
ERS-2 / RA	Apr 1995 - Jun 2003	13.8	330	1.3	35
Envisat / RA-2	Mar 2002 - Apr 2012	13.6 3.2	320 160	1.3 5.5	35
SARAL / AltiKa	Feb 2013 -	35	100	0.6	35
CryoSat-2 / SIRAL	Apr 2010 -	13.6	320	1.08 x 1.2	369
Sentinel-3A / SRAL	Feb 2016 -	13.6 5.4	350 320	1.35 3.4	27
Sentinel-3B / SRAL	Apr 2018 -	13.6 5.4	350 320	1.35 3.4	27

Figure 7 Ocean-Monitoring Satellites (Quartly et al.)

The accuracy of the sea level measurement has improved significantly, as highlighted by Bašić and Bašić (2023) and Srinivasan & Tsonotos (2023) that it has shown an improvement in the accuracy of sea surface height data from 1-2 meters at the inception of altimeter satellite missions to 2-3 centimetres at present (See Table 3). This accuracy is achieved alongside a spatial resolution of approximately 2.5 km and a revisit time of about ten days.

Table 3 Altimetry Satellites (An et al. 2022)

Satellite	Time frame	Revisit period/d	Footprint size/km	Accuracy/CM
Skylab	1973–1974	–	8	85–100
Geos-3	1975–1978	2.3	3.6	25–50
Geosat(GRA)	1985–1990	17	1.7	10–20
ERS-1	1991–2000	335	1.7	10
T/P(Poseidon-2)	1992–2005	10	2.2	6
Envisat	2002–2012	35	1.7	2.5
ICESat	2003–2009	91	0.07	10
Jason-2	Since 2008	10	2.2	2.5–3.4
Cryosat-2	Since 2010	369/30	1.6	1–3
HY-2	Since 2011	168/14	1.9	–
SARAL	Since 2013	35	8	–

Jason-3	Since 2016	10	2.2	2
Sentinel-3	Since 2016	27	0.3	2–8
CFOSAT	Since 2018	13	1.4	–
ICESat-2	Since 2018	91	0.017	3
Jason-CS	Since -2021	21	0.1	–
Sentinel-6	Since -2022	10	0.3	–

However, the altimetry in coastal areas consistently challenges providing reliable data. This is explained by (Grgić et al. 2021) that most satellite altimeter uses radar technology to send and receive radar pulses toward and from the reflected surface area. When the radar pulses are sent to the open ocean, the received waveforms follow a standard wave shape with a steeply rising leading edge and a trailing edge with diminishing power (as seen in Figure 7A examples of returned waveforms).

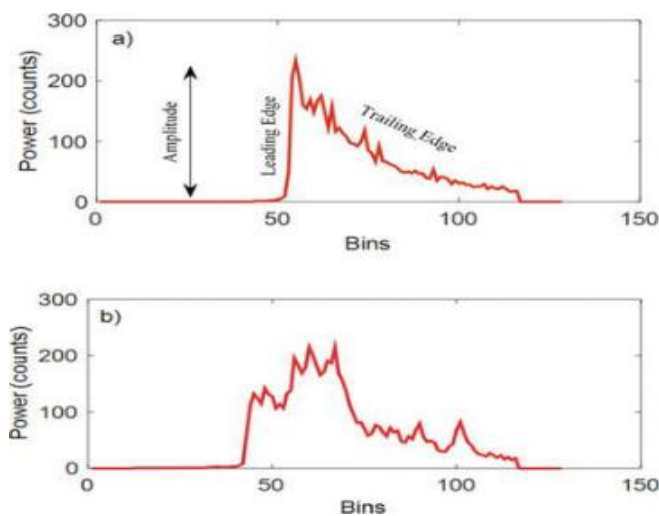


Figure 8(a)Returned waveform over homogeneous ocean surface (b) Returned waveform over complex coastal area. (Bašić, 2023)

However, the accuracy of measurements decreases when the satellite approaches the coastal area, the observation transitions from ocean to land (within 10 km of the coastline), and the radar pulses reflecting the surface area become distorted or contaminated by the inhomogeneity of the surface observed, giving distorted coastal waveforms, this wave appearing in the radar footprint (as seen in the Figure 7B). In addition, coastal altimetry difficulties are caused by various problems, including high-frequency atmospheric signals and tides and challenges in estimating tropospheric corrections (Abdullah et al., 2018). Tracking algorithms have been developed to improve the waveforms for processing; however, retrieving valid data over the last few kilometres to the coastline is still challenging as the contamination starts within 10 km of the coastline.

In summary, while satellite altimetry has made significant strides in monitoring the open ocean and forecasting sea levels, its application in coastal areas remains challenging. Continuous efforts to refine the accuracy of coastal altimetry data are essential for developing effective adaptation and mitigation strategies for coastal communities, emphasising the need for targeted research and technological advancements.

2.1.3 Capabilities and Challenges of Key Sea level Monitoring Missions

The main sea level altimetry missions are Jason 1-3, SARAL/AltiKa, and HY2-A/B. Recent missions such as CryoSat-2 Sentinel-3A and Sentinel-3B have improved the accuracy of measuring sea-level changes. The following table analyses satellite capabilities and challenges of key sea-level monitoring.

Table 4 Capabilities and challenges of key Sea-level and ocean Monitoring Satellites

Satellite	Advantage	limitation
Geosat, Jason-1/2/3, TOPEX/Poseidon, ERS-1/2, Envisat, HY2a/2b	Pioneering Missions to provide open ocean altimetry with high-resolution data for global ocean monitoring small footprint size enhances coastal areas' monitoring of sea-level	limitation on spatial resolution near coastal regions and distorted radar pulse results Data loss due to radar system limitations and single particle radar pulse issues (Jiang et al., 2019)
SARAL/AltiKa - Ka-band	Ka-band altimetry provides finer spatial resolution, minimal ionospheric correction, narrow beamwidth enabling altimetry near land	High sensitivity to clouds and rains, affecting effectiveness in adverse weather and dense vegetation cover (Quartly, Chen 2006a)
CryoSat-2 - Sentinel-3 A/B SAR- Sentinel-6/ Jason-CS SARIn Altimetry	SAR mode improves spatial resolution and lower noise, enhancing coastal and small lake monitoring (McMillan et al. 2018).	SAR mode can have inherent biases and noises that need ongoing identification and calibration. Challenging for coastal areas, (Amani et al. 2022b).
ICESat-1-2	Laser altimetry offers precise measurements as close as 0.9 km to the coastline (Markus et al. 2017).	less atmospheric attenuation and consume more power than radar altimeters (Quartly, Chen 2006). Pose challenge when used on smaller satellites like CubeSats.
Surface Water Ocean Topography (SWOT)	Wide-swath altimetry with high spatial resolution within 1 km from detailed coastal and water bodies (Gower, Barale 2024)	low temporal resolution (21 days) and low revisit time to capture rapid sea-level changes and water dynamics, higher-resolution data is challenging to interpret and requires data classification (Fu et al. 2024).

2.1.4 Applications GNSS Reflectometry for Sea Level Measurement

The Global Navigation Satellite System (GNSS) satellites are used for navigation to determine the accurate position and time on the earth globally, offering both absolute and relative positioning. Various GNSS systems are available globally, as seen in Figure 9, opening a free accessible signal source for various applications and observation, improving the spatial-temporal sampling efficiency of the GNSS monitoring systems (LI et al. 2021).







GPS	GLONASS	Galileo	Beidou	QZSS	NavIC
					
L1, L1C: 1.57 GHz L2C, L2P/Y: 1.23 GHz L5: 1.15 GHz	L1C/A, L1P: 1.60 GHz L2C/A, L2P: 1.25 GHz L3: 1.20 GHz	E1: 1.57 GHz E5A/B, E5AltBOC: 1.19 GHz E6: 1.25 GHz	B1, B1C: 1.57 GHz B2, B2A, B2B: 1.21 GHz B3: 1.27GHz	L1C/A, L1C, L1S: 1.57 GHz L2C: 1.23 GHz L5: 1.18 GHz L6: 1.28 GHz	L5: 1.18 GHz S: 2.248 GHz

Figure 9 Global Navigation Satellite System (GNSS) Satellites (McClaren, 2023)

GNSS signal, particularly GNSS reflectometry (GNSS-R) or (Passive Reflectometry and Interferometry System) spaceborne system. This offers a low-cost passive remote-sensing space technique with a bistatic passive radar method that processes the forward scattered GNSS signals using a receiver. The advantage of using a GNSS signal for sea-level monitoring is that the signal can reach the earth's geoid surface, and the sea level can be measured up to the earth's geoid surface height level (See Figure 2 and 10). The GNSS-R satellite receiver offers global coverage sea level measurement, which depends on the selected orbit, and the spatial resolution ranges from 1 km to hundreds of kilometres, depending on the surface scattering properties of the surface observed (Gao et al. 2018).

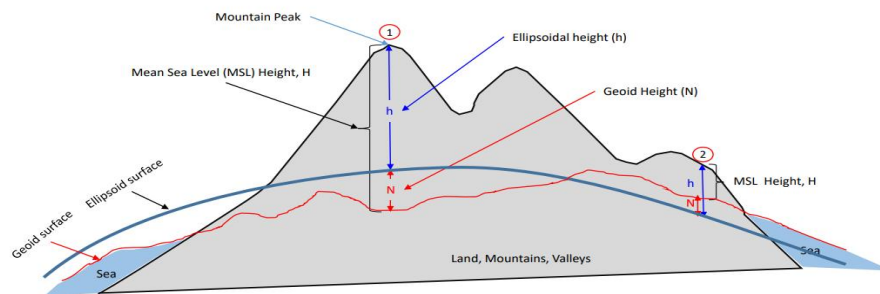


Figure 10 Geoid Height

(Rodriguez-Alvarez et al. 2023) explains, that GNSS-R observation involves the GNSS satellites transmitting signals, the signal scattering off the Earth's surface, and the receiver receiving both the signal coming directly from the source and the signal reflected from the Earth's surface satellites.

This enables the measurement of the height difference between the receiver and the reflecting surface. The sea level measurement can be extracted from the distances between the transmitter, receiver, and surface, such as the sea or ocean (Jin et al., 2024). Both (Gao et al. 2018) and (Xing et al. 2022) pointed out that the GNSS-R sea level observations are conducted in low Earth orbit (LEO), focusing on specular reflection points between GNSS transmitters and the receivers.

However, it is challenging to design a receiver that can receive all the specular reflection signals because of the size and location of the GNSS-R antenna (see figure 11), and the available reflected signal from the ground influences it. Therefore, to improve this the LEO satellites/ the receiver needs to be positioned where the GNSS signal can be received constantly.

For spaceborne receiver, (Bussy-Virat et al. 2019) propose that all the critical parameters for mission design for obtaining the required performance include the number of satellites, the number of orbit planes, relative orientation, and inclination need to be optimised with respect of the GNSS signal and receivers.

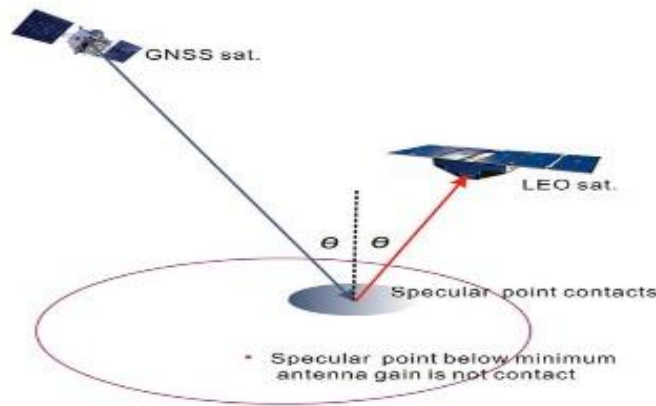


Figure 11 Specular Point of the measured surface (Han, Luo and Xu, 2019)

The distance between the satellite and the receiver can be measured using Carrier-Phase Measurement and signal-to-noise-ratio (SNR) estimation; the Carrier-Phase can provide accuracy up to a centimetre level. The received SNR Signal is a key parameter used to assess the quality of the received signal and expressed in squared amplitude; a higher SNR usually has better signal accuracy, resulting in a higher accurate altimetry.

To achieve the centimetre level accuracy and effectively capture the reflected signal around the receiver, a dual antenna configuration is recommended by (Zhang et al., 2024b) by using a nadir-oriented left-hand circularly polarised (LHCP) antenna direction architecture for reflected signals and receiving capturing direct signals through an RHCP antenna oriented to the zenith with broader beamwidth(See Figure 12).

SNR altimetry can have delays and errors caused by satellite and space-related such as tropospheric and ionospheric errors. The changing of the sea surface and the roughness of the sea surface can impact the accuracy of the altimetry. (Xu et al., 2024) recommend that a baseband signal processing algorithm be integrated into the receiver to improve the accuracy and capture weakened reflected signals. In addition, receiver-related errors can be caused by different configurations of front-end receivers and the characteristics of GNSS signals. This is particularly important when the receiver is designed for more than one type of signal. To overcome this (Liu et al., 2021) recommend that the receiver cross-correlated the locally generated replica of the transmission signal with the reflected signal for a specific time. The receiver needs to use structured GNSS signals, e.g. L1C, L2C, L5 of GPS, B1I, B1C, and B2a of BDS-3, while considering the compensation of the frequency shifts.

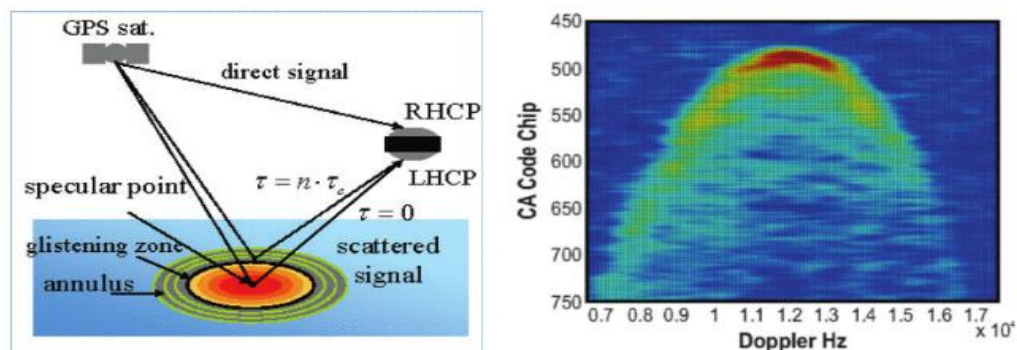


Figure 12 GNSS Signal Propagation and Scattering SNR measurement (Ruf et al., 2012)

The sea level measurement using GNSS-R can effectively improve and overcome that limitation to improve the coastal area. GNSS signals have better weather attenuation and a smaller footprint of GNSS-R signals than traditional radar altimeters. This allows more precise measurements closer to the coast and reduces signal distortion when the signal reaches the coastal area. For example, (Asharaf et al. 2021) explained that the CyGNSS mission has used GNSS-R technology and offered a significant advantage over the Ku-band, which is prone to signal distortion or degradation in rainy seasons, restricting its use in tropical areas.

Therefore, the GNSS-R technology bridges the gap of the flaws in traditional remote sensing as the system can work in all weather conditions, making it a large-scale, low-cost, high-spatial-resolution surface observation possible. Its advantage is that it performs independently without needing ongoing calibration. The L-band has a better attenuation in the cloud and rain than the Ku, X, and C bands used in traditional radar, enabling remote sensing possible even in extreme weather such as typhoons (Xing et al. 2022).

2.1.5 GNSS Reflectometry Missions for Sea Level Measurement

Satellite altimetry has a trade-off between spatial resolution and temporal frequency. The coastal zone has specific needs regarding spatial resolution due to coastal effects and temporal resolution due to short-term events. Also, obtaining accurate coastal or proximity to the coast altimetry has been challenging, mainly due to the footprint contamination of radar technology by land surfaces. Missions with GNSS-R payload have been groundbreaking in acquiring SLR data with high spatial resolution and temporal frequency compared to radar-based technology (Asharaf et al. 2021).

Various satellite missions have been operating, and the requirements are partially achieved by the second-generation CYGNSS and Sentinel six missions, improving the coastal altimetry by getting closer to the coast, typically up to 1–5 km. Despite the improvement, the land contamination for Cryosat-2 begins to affect at 2 km from the coastal area, and this presents significant challenges for accurate sea level monitoring near coastal regions (Amani et al. 2022b). However, the CyGNSS mission with eight satellites working together in a constellation. It has contributed significantly to applying GNSS-R payload for multi-satellite increasing spatial and temporal frequency (every 12 hours) with an accuracy of 1-2 cm see table (Gao et al. 2018). The BuFeng-1A/1B mission has a spatial resolution of about 50 km and an accuracy of 5-10 cm; while the CYGNSS provides more frequent data, the BuFeng-1A/1B mission offers broader spatial coverage. Table 5 shows the primary GNSS-R mission with revisit time and accuracy.

Table 5 GNSS-R Missions

Mission Name	Satellite Type	Orbit Type	Payload	Revisit Period	Footprint Size	Accuracy	Inclination
UK-DMC 1	Micro-satellite	Sun-Synchronous Orbit	Optical multispectral imagers	1-2 days	~600 km	N/A	~98°
TechDemo Sat-1	Micro-satellite	Sun-Synchronous Orbit	GNSS-R receiver, radiation monitor	1-2 days	~20 km	~5-10 cm	~98°
CYGNUS	Micro-satellite	LEO	GNSS-R receiver	12 hours	~25 km	~1-2 cm	~35°
WNISAT-1R	Micro-satellite	LEO	Optical imager GNSS-R receiver	1-2 days	~100 km	~10 cm	~98°
BuFeng-1A/1B	Micro-satellite	LEO	GNSS-R receiver	One day	~50 km	~5-10 cm	~35°
UK-DOT-1	Micro-satellite	Sun-Synchronous Orbit	technology demonstrators	N/A	N/A	N/A	~98°
FSSCat	CubeSat (6U)	Sun-Synchronous Orbit	GNSS-R receiver, multispectral imager	1-2 days	~15 km	~10 cm	~97.6°
FengYun-3E	CubeSat	Polar Orbit	GNSS-R receiver meteorological instruments	Daily	~20 km	~2-5 cm	~98.75°
HydroGNSS	CubeSat (6U)	Sun-Synchronous Orbit	GNSS-R receiver	1-2 days	~20 km	~1-2 cm	~98°

2.2 GNSS-R Technology for CubeSats

2.2.1 CubeSats for Sea Level Monitoring

Satellite building for space missions is a long process and is challenging. However, in the last 10-15 years, the CubeSat development has changed the space industry, and as a result, more missions have been able to operate. CubeSats are small satellites with compact subsystems that have the typical satellite characteristics; CubeSats and its subsystems are compact and can be assembled using in-house built subsystems or bought from suppliers, also known as Commercial-Off-The-Shelf (COTS) (Cheong et al. 2020). The initial sizes for the CubeSats were cube-shaped, measuring $10 \times 10 \times 10$ cm, referred to as 1U, and weighing around 1 to 1-1/3 kilograms. They can be built in diverse sizes (See Figure 13)(Loff 2018).

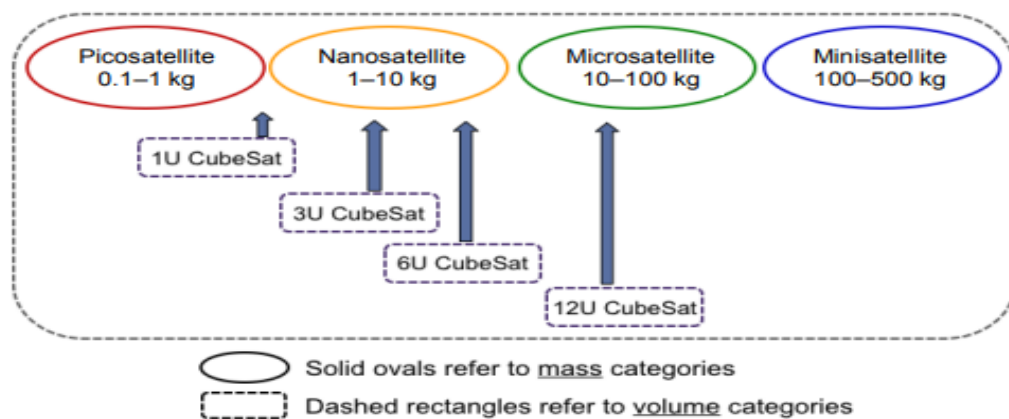


Figure 13 CubeSats Sizes (Venturini 2017)

In recent years, CubeSats have emerged as a technology enabler, facilitating the development of small satellites through the miniaturisation of sensor technologies. They have also played a significant role in revolutionizing earth observation in academia, particularly in research and teaching space missions. A study by (Santilli et al. 2018) found that CubeSat missions can effectively monitor sea levels by implementing an optimized architecture design to maintain the performance of CubeSat and COTS systems, offering sea level monitoring capabilities like larger platforms. Since 2010, the launch has concentrated on low earth orbit (LEO) as they provide various data collection methods, such as atmospheric remote sensing, including GNSS-R payloads (Burkhard, Weston 2021).

Despite the progress, CubeSat has higher failure rates than traditional satellites. The causes of those failures are design flaws, materials failures, extreme conditions or environments, and, most commonly, human factors, including accidents(See Figure 14). This is because using COTS products has implications for CubeSat's reliability, availabilities, and redundancies, as each manufacturer has its own rating and qualification level standard. Hence, extensive testing, verification, and validation are required when using CubeSat. Therefore, by implementing the necessary testing and validation, CubeSat with GNSS-R payload can provide enhanced spatial and temporal coverage at a reduced cost compared to traditional active radar nadir or wide-swath altimetry.

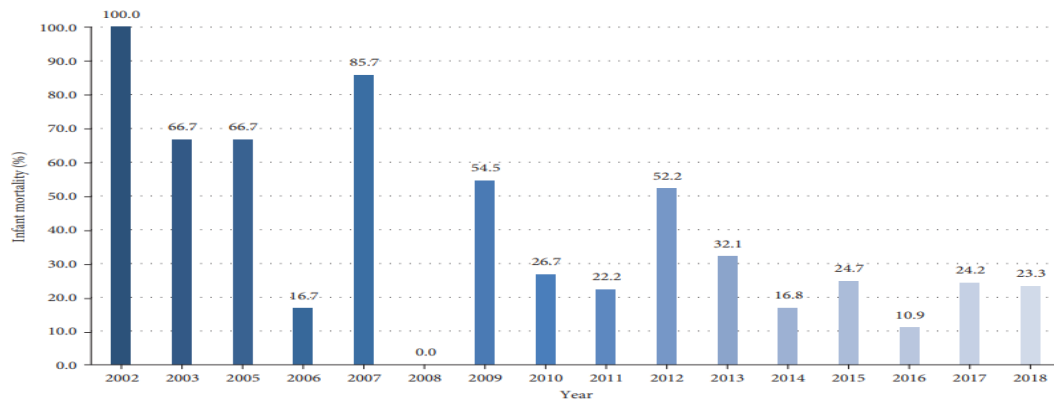


FIGURE 9: Infant mortality for CubeSats from 2002 up to May 31, 2018 (launch failures excluded).

Figure 14 CubeSat failure (Villela et al. 2019)

The coastal environment is dynamic and requires continuous observations over time. Research conducted by (Quartly Chen 2006b) and (Zhang et al. 2024b) showed that one Satellite alone cannot obtain the spatial-temporal altimetry required to monitor the sea level. Using identical small multiple satellites and deploying at the same orbital plane can achieve consistent spatial and temporal altimetry, and uninterrupted observation. Thus, meeting the requirement for sea level monitoring while reducing the cost of the mission.

2.3 Evaluation of Current Limitations in Sea Level Monitoring

The literature review discusses advancements in sea level monitoring; it has evaluated various historical satellite altimetry and the new low-cost GNSS-R missions. Both historical and current missions, such as Sentinel-6 and AltiKa, have been providing sea level measurements near coastal areas with better accuracy and close coastal area measurements. The AltiKa mission has contributed to achieving finer spatial resolution by introducing a small satellite with narrow beam widths, reducing footprint sizes to as little as 1 km, and improving vertical resolution to approximately 0.3 meters. The Ka-band radar is highly sensitive to atmospheric conditions such as clouds and rain, further distorting the altimeter near the coastal area. This issue impacts the accuracy of sea level measurements, highlighting the need for further research in this area (Vignudelli et al., 2019).

It was highlighted that the GNSS-R for sea level measurement showed suitability for monitoring long-term sea conditions. For example, the CYGNSS, BuFeng-1A/1B and FSSCat, “Federated Satellite Systems/ 3 Cat-5” missions have demonstrated the ability to provide continuous, detailed altimetry. This shows that GNSS-R altimetry can be an alternative to improve the accuracy of coastal altimeters and the spatial and temporal resolution required for sea-level monitoring.

However, despite improvements in the GNSS-R, some improvements still need to be overcome to improve coastal altimetry. For example, land contamination in the Cryosat-2 mission begins to affect only 2 km from the coast, and it has also presented significant challenges for ongoing calibration (Amani et al. 2022b). Despite this, the CYGNSS mission has successfully improved the spatial and temporal resolution using 8 CubeSat constellations. This has instilled confidence in the progress of the GNSS-R mission, as the GNSS-R-based SSH altimetry technique provides the possibility to measure mesoscale sea-surface height using constellations. The FSSCat mission has demonstrated the implementation of artificial intelligence (AI) experiments for discarding cloudy images.

Therefore, using both missions as a base and taking this further, for this mission, the AI application is vital for improving the real-time processing and optimising the data collection of the sea level will be implemented. This can be achieved using a wider beam width and receiving more signals from different GNSS systems to provide more available reflections. In addition, the signal processing algorithms need further optimisation and refinement to maximise GNSS-R measurements' observation capacity and accuracy. As the gap analysis highlighted, improving the algorithm is vital for this mission. The ionospheric delay error is still a limitation and is regarded as the primary systematic error source.

To achieve high spatial and temporal resolution, the project will evaluate the number of satellites and revisit time, including the critical role of effective mission design in obtaining the GNSS-R observations and selecting specific mission parameters tailored to targeted specular points, including instrument configurations and orbital parameters (Gao et al. 2018). To optimising and improve the spatial and temporal resolution of GNSS-R observations

3. Methodology

The literature review research has highlighted that GNSS-R altimetry can be used with CubeSats to achieve high spatial and temporal resolution for sea-level monitoring. The following methodology work will study the design and configuration of CubeSat with GNSS-R payload. The CubeSat will operate in a Low Earth Orbit (LEO) under the GNSS satellites to enable the GNSS-R receiver to acquire a signal from GNSS satellites accurately. This LEO orbit is significant as it allows the CubeSat to be near the GNSS satellites, ensuring a strong and reliable signal acquisition. The key drivers for this mission are the spatial and temporal resolutions; this will increase the accuracy of the seal level measurement near the coastal area. The Mission's key drivers will influence the choice of elements and subsystems. The CubeSat subsystems and orbit selection are taken by considering the cost and time of the development for overall mission cost savings, as these factors are crucial in ensuring the feasibility and success of the mission. The methodology for this project will adhere to the ECSS-(ECSS--M--30--01A) (European Cooperation for Space Standardization) design philosophies for the entire system. The ECSS standard is a comprehensive framework that ensures consistency in space development, covering all aspects and stages of the project milestones. This project will align with industry best practices by following the ECSS standards, enhancing its credibility and reliability.

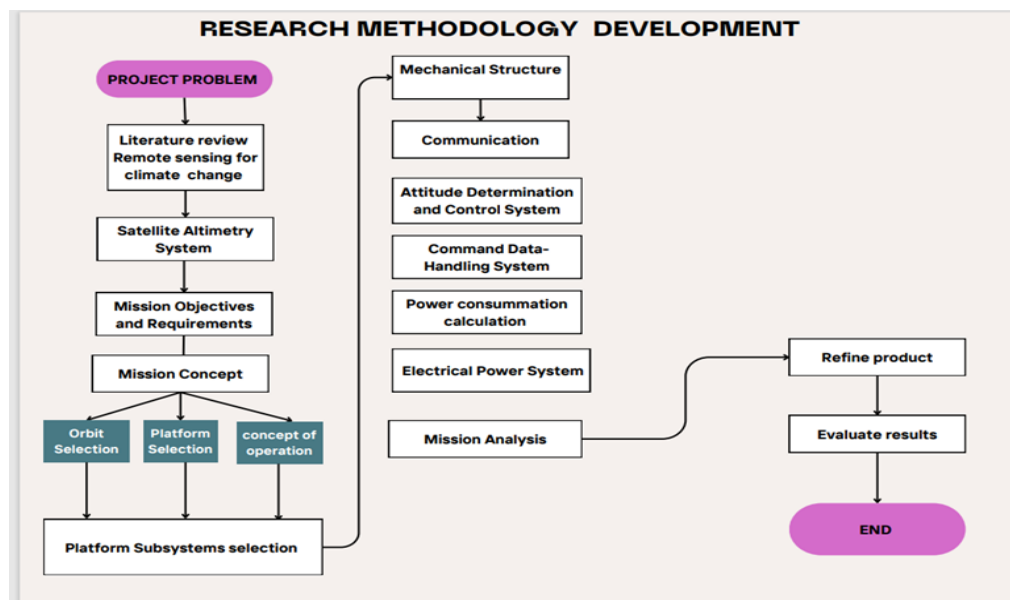


Figure 15 Research Process

European Cooperation for Space Standardization Design Philosophies (ECSS-M-30-01A)



Figure 16 ECSS-(ECSS--M--30--01A) Standard Space Project Management

3.1 Methodology Implementation Process

The following Methodology focuses on the ECSS standard Phases 0 and A, which will fulfil the mission concept, objective and top-level requirements. The methodology workflow is shown on figure 17.

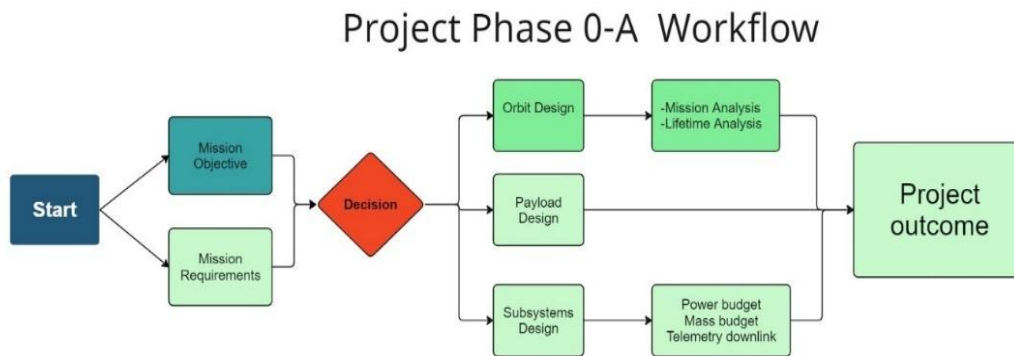


Figure 17 Phase 0- A workflow.

3.1.1 Orbital Parameters Requirements

The constraint for the mission is selecting a suitable altitude and orbit in which the observation area is located on the specular reflection point between the GNSS satellites and the satellites. GNSS-R missions' inclination is the critical parameter affecting the mission's coverage, altitude, and average revisit time with their accuracy. Therefore, the orbital selection for this mission shall consider critical factors, including altitude, inclination, and the configuration of the satellites, to achieve the primary requirements of the mission. The orbital selection for the mission will influence the accuracy and ability to measure the sea level by using the GNSS-R receiver; if the orbit is too high above the GNSS satellite signal, the receiver will receive fewer GNSS signals. (Tan et al. 2023) advises that selecting the orbital position for the LEO-based GNSS receiver should involve careful consideration of high-quality reflected signals. This can be achieved by configuring the elevation beamwidth and azimuth beamwidth of the off-nadir LHCP antenna on the LEO-based GNSS receiver to maintain high antenna gain for the reflected signal. Table 6 shows the orbit selection criteria and the considerations taken during the orbital calculation. Based on the literature review, various inclinations and revisit times have been evaluated as factors in the selection process.

Table 6 Orbital selection criteria

Orbit Selection Requirements Criteria	Influencing factors affect the orbit selection	Orbital Parameter considered
Observation frequency	Swath width, revisit time	Altitude
Global access	Maximum latitude; spacing between ground-tracks	Inclination, altitude
Regular ground pattern	Synchronous or drafting orbit	Altitude
Continuous illumination	Sun Synchronous	Inclination, altitude
Instrument special resolution		Altitude
Mission lifetime	Orbital decay	Altitude
Accessibility for GNSS signal	specular reflection point	inclination and altitude

3.1.2 GNSS-R Payload and Altimeter System Requirement

Based on past mission analyses and the need for coastal sea level measurement, this mission will aim to achieve the following (see table)accuracy and revisit time. This target will improve the spatial and temporal resolutions.

Table 7 Mission Metrics

Metric	Value
Accuracy	~1-2 cm
Revisit Period	1-2 days

3.1.3 Preliminary System Requirements and System Design

The preliminary system and subsystem requirements are identified by analysing the lessons learnt from the past mission. The reference missions are from the FSSCat, “Federated Satellite Systems/ 3 Cat-5”, and the CYGNSS mission. Both have significantly contributed to the advancement of the GNSSR mission.

Table 8 Preliminary Requirements

CubeSat Subsystems	Subsystem Requirements
Structure	The structure of the shall be 6U Size The structure shall support all the subsystem's component placement. The Structure shall ensure all the mechanisms do not fail throughout the mission.
Communication (Antennas and receivers)	The communication subsystem shall ensure communication between the satellite and ground station for the central communication of the Telemetry, Tracking & Control (TT&C). The communication system shall allow up-link and down-link directions communication between the subsystems.
Electrical Power Systems (EPS)	The electric power subsystem shall generate the power required to operate the satellite. The satellite shall have a power supply during eclipse time
Attitude determination and control system controls (ADCS)	The ADCS shall control the orientation of the satellite The ADCS shall estimate the position and attitude of the satellite The ADCS sensors shall resolve three degrees of freedom attitude movement
The command & data handling system (CDHS)	The CDHS shall store payload and spacecraft state of health data. The CDHS shall have high processing speeds and optimal power consumption for extensive data. The CDHS shall execute user command transitions between user-dictated modes of operations. The CDHS shall monitor the health and performance of all subsystems.
On-Board Computer	The on-board computer shall handle large amounts of data. The OBC shall integrate AI to process large data and with high speeds.
Payload	The GNSS-R receiver payload shall be a dual GNSS-R receiver capable of tracking signals from all major satellite navigation systems (GPS, Galileo).

4. Results

4.1 Mission Objectives

This mission aims to monitor global and coastal sea level changes with high spatial and temporal resolution by using the capability of nanosatellites, particularly the 6U size CubeSat standard.

Mission Main Objectives

- 1) The primary mission requirement for the satellite system is to provide accurate measurement near the coastal area and overall continuous sea-level measurement.
- 2) To achieve high spatial and temporal resolution altimetric precision near the coastal area using GNSS-R Signal comparable to successful missions such as CYGNSS, FSSCat- CubeSat (6U).
- 3) To evaluate the improvement of accuracy of coastal sea level Improvement of accuracy near coastline altimetry by using GNSS-R technology
- 4) Monitoring global and coastal sea level changes with high spatial and temporal resolution.

Mission Success Criteria: The following criteria have been completed to evaluate the success and performance of the mission.

Minimum Success Criteria

1. CubeSat successfully deployed in orbit
 2. Communication with the CubeSat established
 3. Payload and telemetry received for the first stage of the mission
- Sufficient:** For half of the duration of the whole mission, telemetry and payload data received
- Desirable:** Received telemetry and payload data for the duration of the whole mission.

4.2 Mission Concept

4.2.1 Orbit Design and Analyses

For the mission, orbit selection should consider appropriate coverage time, visibility with the ground station and eclipse time. The key driver and requirement for the orbit selection is the receiver's ability to receive the scattered and GNSS signals over the target sea surface in a nadir-looking configuration. Hence, (Gao et al. 2018) validated that considering the signal loss on the transmission link, the optimal orbit height for the GNSS-R mission should be set at about 500-550 km (Leo orbit) just under the GNSS signals. The satellite operating in a sun-synchronous orbit (SSO) will allow it to orbit with fixed light at a local time and a stable temperature, and it has a global coverage capacity. This will reduce the design for the temperature variation of the orbit. For this project, the drag and sun's attraction perturbations are neglected as they will be calculated in Phase B. (Ma, Zhai 2004) stated that to fulfil the Sun-synchronous orbits requirement, the following relationship should be fulfilled, i.e. inclination (i), Semi-major axis (a), and Eccentricity (e):

$$d\Omega/dt = -32nJ_2R_p^2\cos i = \dot{\alpha}\theta = 0.9856 \frac{\text{deg}}{\text{day}}$$

The sun-synchronous orbit (SSO) is an orbit easily accessible by commercial launches, as this will be a better option for reducing the cost of the launch and deployment. The following parameters are the proposed orbit for this mission. Hence, sun-synchronous orbit (SSO) is the optimal orbit for this mission to monitor the United Kingdom coastline, with an altitude of around ~550 km. The sun-synchronous orbit (SSO) has a 98-degree of inclination. The following table shows the orbital element

calculation for this mission and the contact time; the steps taken are shown in the appendix. The figure shows the orbital and ground simulation as part of the orbital selection process.

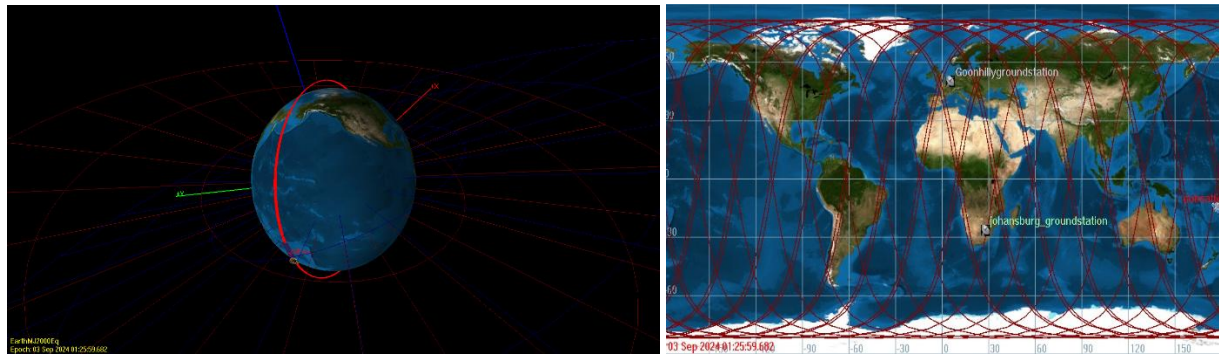


Figure 18 A B satellite operating in a sun-synchronous orbit (SSO) and ground station contacts.

Table 9 Orbital mechanic calculation of the mission

Orbit selection and orbital	Value
Semi-major axis (a)	6,921km
Eccentricity (e)	0
Inclination (i)	98°
Argument of perigee (ω)	0
Right Ascension of Ascending Node (RAAN)	0
Orbital velocity (ΔV)	$7.589 \frac{km}{s}$
orbital energy (ϵ)	$-28.8 \frac{MJ}{kg}$
Orbital period (T)	5777.430s = 9.2 min
Orbital altitude	500-550 km
Number of orbits per day	15

4.2.2 Concept of Operation (In-Orbit Operations)

The satellite has four primary modes of operation to support its mission objectives, culminating in the final disposal event. These modes are launch early operations (LEOP), initial, normal, and safe. The following descriptions are based on the preliminary mission requirements for nominal payload operation, and the table outlines all the mode stages.

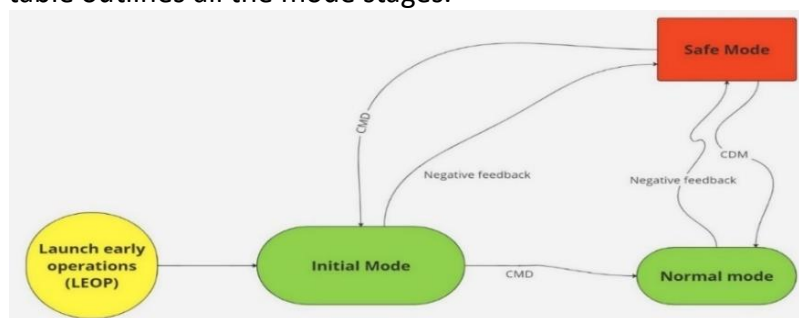


Figure 19 Mission Concept of operation.

Table 10 Mission Operation Mode

Phase	Mission Phase	Description
0	Launch early operations (LEOP)	The LEOP mode starts after the separation from the launch vehicle. Subsystems and instruments are powered on in this mode when the solar panels are stowed.
1	Initial Mode	This mode will allow the EPS to provide power to the system. The command and data-handling system transmits all the housing keeping Telemetry Data (STD). This also allows the Comprehensive satellite subsystem checking. The ground station is activated to enable satellite tracking from the ground.
2	Normal Operation Mode	This mode will allow all the regular operational modes, such as payload data collection, attitude pointing and downlink & uplink for housekeeping. The ground segment will take complete control of scheduling telecommands. When negative feedback occurs during the mission, the normal operation mode will switch to safe mode.
3	Safe (Survival) mode	This mode occurs when the satellite identifies any abnormal activity during the mission. This mode is triggered automatically by onboard software, and all the subsystems will be off except the critical ones, the OBC, the EPS, and the antenna receiver and transmitter.
4	End of mission	End-of-life planning and disposal execution operation

4.2.3 GNSS-R Payload

The GNSS-R payload design will optimise antenna configurations and system integration to ensure accurate sea-level measurements. The primary constraint for the receiver is that the receiver needs to be under all GNSS signals and at an optimal altitude to receive the reflected one. The receiver will have a dual-frequency configuration with a high-gain and high-sensitivity antenna. This will enable fast acquisition and tracking of the GNSS signals received and used signals from the Galileo and GPS GNSS systems. The subsystem will use a standard nadir-looking high-gain dual-frequency left-hand circularly polarised (LHCP) antenna to receive the reflected/scattered signals from GNSS satellites. A low-noise amplifier (LNA) will be installed close to the antenna. The main subsystems of the payload system and its functionality are shown in the diagram and table below. (See appendix E for description)

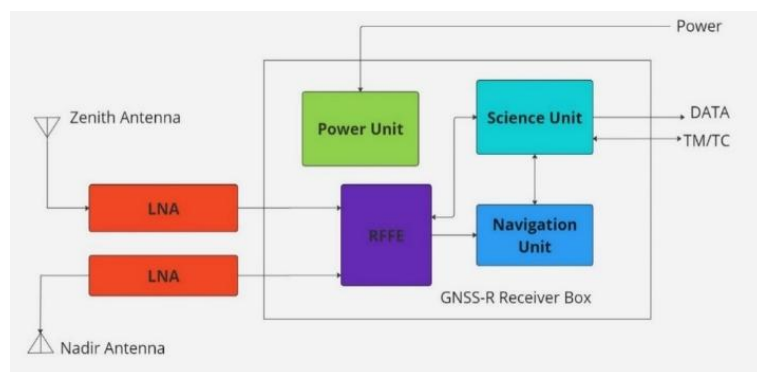


Figure 20 GNSS-R Subsystems

4.2.4 Constellation

The research evaluated that more than one satellite is required to measure the sea level effectively. Past constellation missions studied, e.g., the CYGNSS mission, has eight satellites equally distributed operating to gather within a single orbital plane. (Zhang et al. 2024) stated that by using the Walker-Delta constellations between 4 and 8 satellites, the altimetric precision has improved from 0.3158m to 0.2231m. For this mission, the Walker-Delta constellation design satisfies the requirements, as the constellations are distributed across 360°. It comprises the total number of satellites in circular orbits with the same period and inclination (Han et al. 2014). The calculation performed shows using two orbital planes results in a negative Right Ascension of the Ascending Node (RAAN) change rate. This negative RAAN rate indicates that the constellation configuration would not be feasible with two planes. Therefore, all the satellites will be placed on a single orbital plane, and the distance between them will be 45°. (See appendix C for calculation)

$$spacing = \frac{360^\circ}{\text{number of satellites per plane}} \quad spacing = \frac{360^\circ}{8} = 45^\circ$$

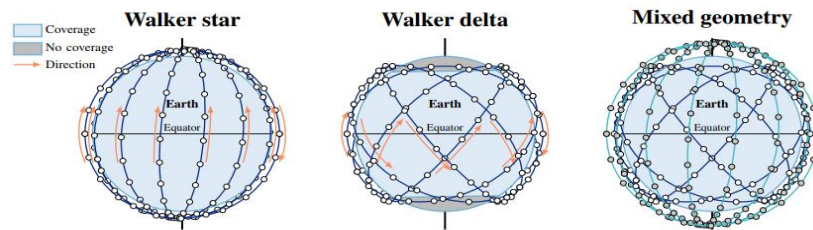


Figure 21 Constellation Design (Leyva-Mayorga et al., 2022)

4.3 Mission Analysis

The average CubeSat mission in a Low Earth Orbit (LEO) typically lasts 2-5 years. Factors such as solar radiation pressure, atmospheric drag, orbital decay, power degradation, Earth gravity, orbit configuration, satellite mass, and drag area all impact CubeSat's lifetime. The effect of drag on the satellite, depending on its shape and orientation, the maximum value of drag coefficient 2 and 2.2, with a drag area of 0.036 m² used for analysis. The results are summarised below for lifetime and access time.

4.3.1 Lifetime Analysis

GMAT software is used to analyse the spacecraft's lifetime; the input required for these analyses are spacecraft dry mass, drag area, and atmospheric drag. The GMAT and satellite lifetime calculation is executed to analyse how long the satellite decays to an altitude of 180km. The results showed the satellite takes almost 70 elapsed days to decay to 180 – 200 km altitude. This is a preliminary calculation, and Further analyses and mission optimisation can improve this.

Table 11 Lifetime analysis

Input	Value
Spacecraft Mass	6-8 kg
Drag coefficient (Cd)	2.2
Drag area	0.036m ²
Orbit decay altitude	180km

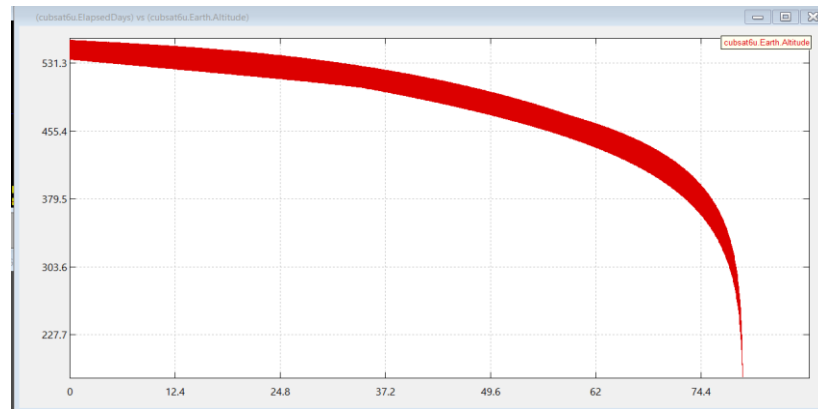


Figure 22 Lifetime analysis of GMAT simulation.

4.3.2 Access Time Analysis

Satellite access time analysis provides the mission's access time to the ground station; it is analysed during the mission planning process. This analysis is crucial for understanding the satellite and ground station contact time. For this mission, the ground stations selected are the Goonhilly and Johannesburg. The Goonhilly ground station supports the S-band downlink. Johannesburg ground station was selected to observe contact time in different regions, and eclipse times for the mission will be analysed. This allows us to examine the downlink and uplink time for the science data generated. The eclipse time analysis enables us to evaluate the total time the satellite will go to the eclipse and the time it spends in the Umbria (the darkest part of a shadow) and penumbra (the partially shaded outer region of a shadow); this is vital for calculating the power budget. The result showed that for the 7-day simulation results week mission, the satellite had on average, 10 min contact time with the Goonhilly ground station and 5.69 min on average with the Johannesburg. The Eclipse analyses show that the satellite umbra and penumbra time in seconds (see figure below)

Target: cubsat6u				Observer: johansburg_groundstation			
Observer: Goonhillygroundstation		Start Time (UTC)		Duration (s)	Start Time (UTC)		Duration (s)
01 Sep 2024	14:04:05.165	01 Sep 2024	14:13:17.962	552.79655118	04 Sep 2024	22:32:30.715	167.39165392
03 Sep 2024	00:42:37.903	03 Sep 2024	00:52:01.189	563.28646895	06 Sep 2024	12:05:06.383	360.61960371
03 Sep 2024	23:00:42.012	03 Sep 2024	23:08:07.297	445.28551443	07 Sep 2024	10:20:59.597	392.46555506
06 Sep 2024	14:53:56.089	06 Sep 2024	15:01:10.841	434.75167465	10 Sep 2024	00:51:13.805	255.92354208
08 Sep 2024	01:31:27.014	08 Sep 2024	01:38:55.762	448.74748645	10 Sep 2024	23:05:06.607	456.12439492
08 Sep 2024	23:45:57.942	08 Sep 2024	23:55:07.155	549.21348968	12 Sep 2024	11:01:57.565	514.05919937
11 Sep 2024	15:38:50.369	11 Sep 2024	15:41:34.917	164.58481440	12 Sep 2024	11:10:31.625	514.05919937
12 Sep 2024	13:51:17.232	12 Sep 2024	14:00:36.931	559.69827741	16 Sep 2024	23:30:01.815	513.02806309
13 Sep 2024	12:07:07.964	13 Sep 2024	12:12:48.067	340.10350064	19 Sep 2024	11:11:53.455	514.37369959
14 Sep 2024	02:03:23.869	14 Sep 2024	02:07:42.611	258.74168869	23 Sep 2024	23:30:33.636	505.77316034
15 Sep 2024	00:14:18.844	15 Sep 2024	00:23:45.529	566.68480943	27 Sep 2024	10:51:33.244	482.34383032
15 Sep 2024	22:31:40.215	15 Sep 2024	22:35:55.668	255.45340532	02 Oct 2024	00:31:36.801	415.06126458
19 Sep 2024	14:01:05.039	19 Sep 2024	14:10:12.597	547.55857259	03 Oct 2024	00:13:34.112	476.72569166
20 Sep 2024	12:14:47.210	20 Sep 2024	12:20:57.942	370.73215039	07 Oct 2024	11:02:36.477	490.27316426
21 Sep 2024	02:10:44.144	21 Sep 2024	02:13:48.370	184.22602970	08 Oct 2024	10:43:10.477	437.02533996
22 Sep 2024	00:19:04.125	22 Sep 2024	00:28:25.151	561.02550442	09 Oct 2024	10:23:51.967	320.42760436
22 Sep 2024	22:34:26.016	22 Sep 2024	22:38:36.113	250.09685716	29 Oct 2024	10:53:30.532	414.23336472
26 Sep 2024	13:55:40.152	26 Sep 2024	14:04:48.344	548.19167334	30 Oct 2024	11:51:54.221	438.18187664
27 Sep 2024	13:40:04.679	27 Sep 2024	13:49:18.151	553.47135955	01 Nov 2024	23:41:55.421	438.34724488
29 Sep 2024	01:43:31.457	29 Sep 2024	01:50:08.742	397.28558210	03 Nov 2024	00:37:16.885	376.12203296
29 Sep 2024	23:51:43.662	30 Sep 2024	00:00:33.333	529.67175550	06 Nov 2024	10:32:08.788	205.19544329
30 Sep 2024	23:35:14.793	30 Sep 2024	23:43:33.280	459.30740264	09 Nov 2024	01:04:23.806	165.23138538
06 Oct 2024	15:47:03.140	06 Oct 2024	15:48:14.226	71.085546585	14 Nov 2024	11:35:28.109	411.66783756
07 Oct 2024	13:50:49.233	07 Oct 2024	13:59:52.480	543.24630594			
08 Oct 2024	13:30:48.348	08 Oct 2024	13:39:49.652	541.30387312			
09 Oct 2024	13:10:26.251	09 Oct 2024	13:19:06.163	519.91182303			
13 Oct 2024	01:56:16.063	13 Oct 2024	02:01:43.957	327.89368266			
14 Oct 2024	01:32:21.877	14 Oct 2024	01:39:41.656	439.81932029			
15 Oct 2024	01:08:25.859	15 Oct 2024	01:16:46.735	500.87586694			
16 Oct 2024	00:44:18.338	16 Oct 2024	00:53:07.296	528.95864141			
17 Oct 2024	00:19:55.913	17 Oct 2024	00:28:45.415	529.50277319			
17 Oct 2024	23:55:17.659	18 Oct 2024	00:03:40.718	503.05843425			
18 Oct 2024	23:30:24.828	18 Oct 2024	23:37:50.708	445.88020606			
19 Oct 2024	23:05:23.127	19 Oct 2024	23:11:08.446	345.31867176			
21 Oct 2024	00:09:56.242	21 Oct 2024	00:18:31.644	515.40200383			
21 Oct 2024	00:09:56.242	21 Oct 2024	00:18:31.644	515.40200383			

Number of events : 22

Figure 23A-B Access time Results.

4.4 Satellite Subsystem Design

4.4.1 Platform

Existing missions were evaluated, and 6U CubeSat was deemed the acceptance size for this mission. The mission will be a 6U CubeSat made from a space-graded aluminium alloy, as seen in Figure 25 in a similar 6U CubeSat mission in orbit. The satellite bus will consist of communication, mechanical, power, command and data handling, attitude determination, and control subsystems. The following diagram and table show the top-level system architecture and the interface and functionality of the subsystem's characteristics.

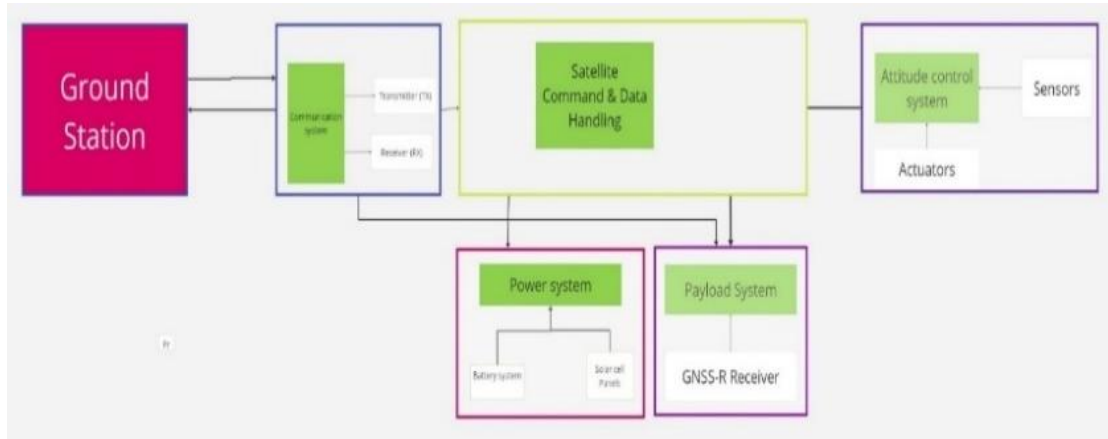


Figure 24 Top Level System interface.



Figure 25 FSSCat 6U CubeSat Mission (Tyvak 2020)

Table 12 Satellite characteristic

Satellite Characteristics	
Satellite structure size	100x226. 3x366 mm (6U CubeSat)
Dry Mass structure	850 g (including fasteners, switches and two mounted rings).
Solar array	Two deployable solar array panels
Deployer	commercially available deployer and another mechanical interface.

4.4.2 Communication

The Communication Subsystem facilitates continuous communication between the satellite and ground stations for Telemetry, Tracking, and Control (TTC). A GMAT simulation was conducted at two ground stations to evaluate the satellite's contact time. The results, which show an average of 10 minutes of contact time with the Goonhilly ground station over a month, align with the expected 15-minute contact time for a typical Leo high inclination.

Table 13 Ground Station Contact

	Goonhilly Ground Station	Johannesburg
Number of Events	52	22
Duration of Contacts	71 -566 seconds	165 -514 seconds
Antenna band	S, C, X, Ku	UHF/VHF

Considering the high data range required for this mission, the Honeywell S-Band STC-MS03 transceiver has been selected as an S-band that will benefit science data downlink (Honeywell 2024). The advantage of this transceiver is that it has a low power usage and weight. For this project, the Free-Space Path Loss (FSPL) and Receiver Sensitivity (P_r) calculations are ignored, as they will be calculated in phase B. The S-band Patch Antenna with a wide FOV of 120 degrees enables a high field during the satellite operation, which is selected to complement the antenna with the transceiver. (Ecuadorian Civilian Space Agency, 2007) A data rate calculation was performed to validate the selection of the transceiver and to see if it satisfied the requirement. The CYGNSS mission data rate per day of 4 Mbit/s with the selected transceiver maximum Rx data showed that the transceiver could transfer up to 405.3 Mb per pass.

Table 14 Data rate calculation

Parameter	Information	Evaluation
Downlink Data CYGNSS data rate per day	4 Mbit/s	
Uplink Data CYGNSS data rate per day	2 kbit/s	
DATA RATES-Band Transceiver	~6.25 Mbit/s (QPSK/OQPSK) ~1.024 Mbit/s (BPSK)	
Transceiver Rx Frequency Range	2025 to 2120 MHz	The Transceiver supports up to 6.25 Mbit/s
Transceiver-Tx Frequency Range	2200 to 2290 MHz	The transceiver supports up to 1.024 Mbit/s
Bandwidth S-Band Patch Antenna	2025 to 2120 MHz 2200 to 2300 MHz	
Data Transferred= Data Rate Duration* downlink data/uplinkdata	6.25 Mbit/s \times 552.8 s = 3,445,000,000 bits \approx 405.3 MB	The data rate calculation shows that it can transfer up to 405.3 MB of data per pass



Figure 26 A, B Transceiver and Antenna

4.4.3 Attitude Determination and Control Subsystem and On-Board Computer(OBC)

The Attitude Determination and Control System (ADCS) for this mission is required for the spacecraft's orientation and for pointing the nadir. The on-board computer (OBC) is responsible for processing commands and all the other systems, including the payload. The GNSS sensor is used for orbit determination. The ADCs have three modes: Detumbling mode, nadir pointing (nominal mode), and vertical mode, maintaining the orientation and control of the earth pointing system to ensure that the GNSS-R receiver receives the reflected signal. The ADCS used for the modes are

1. Detumble Mode
 - Sensors: three-axis control, three reaction wheels and three magnetometers
2. Sun Point Mode:
 - Sensors: Integrated Sun sensors and Interface external star tracker
3. Vertical Mode
 - Sensors: Earth sensor

The fully integrated autonomous ADCS from AAC Clyde Space (iADCS400) will be used. It allows the integration of the OBC processor system and further needed GNSS sensors for orbit determination. It is fully autonomous, which will reduce further mission-specific tasks and data processing. Using this ADCS will reduce mass and cost reduction, as well as system integration errors, as they are from the same manufacturers and are fully integrated.

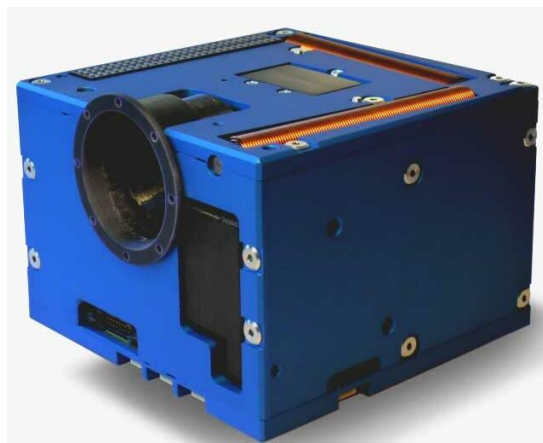


Figure 27 ADCS AAC Clyde Space (iADCS400) (AC Clyde Space 2021).

4.4.4 Electrical Power System (EPS)

The role of the Electrical Power Subsystem (EPS) is power generation, power storage, and power distribution. The EPS subsystems are the solar panel, EPS board and battery. During the day, solar power will generate and recharge the Latium battery, and the stored power will be used during the eclipse. The payload requires 40% of the power to receive and process the GNSS signals. Therefore, the SSO orbit will allow a fixed light at a local time and a stable temperature. This will charge the charged battery used during the eclipse time. This preliminary power budget calculation is obtained from Space Mission Engineering (James Richard Wertz et al.). Based on the calculation obtained, CubeSat requires up to 36.66w, using this calculation as a baseline, the Endurasat two solar panels with a 70% ratio can generate a capacity of 38.4w and meet power budget requirements. This power requirement will ensure the satellite has enough power during nominal and safe operational modes. For battery storage, the CubeSat need approximately 1.03Wh, and the EXA BA0x High Capacity can supply the required capacity as it has up to 22.2Wh capacity and is also lightweight, around 125 g. All the calculations obtained are annexed to Appendix E.

Table 15 Power Budget Calculation

CubeSat Subsystems	Normal Operation Mode		Power Needed during the Mode	
	% Operating power consumption	Power Requirement (W)	Normal Mode Duty	Safe Mode Duty use less power
Communication	5%	1.833	ON	ON
Power Systems (EPS)	30%	10.99	ON	ON
ADCS	15%	5.49	ON	ON/
Command & Data Handling System (CDHS)	5%	1.833	ON	ON
On-Board Computer	5%	1.833	ON	ON
Payload	40%	14.66	ON	OFF
Total	100%	36.8		

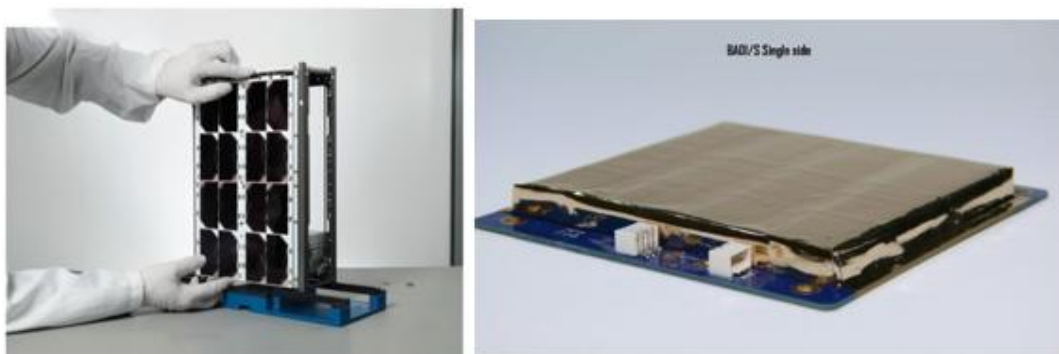


Figure 28 Selected solar panels and Battery. (Endurasat, 2024)

4.4.5 Mass Budgets

For preliminary calculation for mass budget, the suppliers' mass was calculated as it is used for the simulation input. The total Dry mass for the CubeSat is approximately 5.2 kg with a 5% margin. However, this will change as this preliminary design and calculation of the mass budget calculation is taken from The New SMAD (James Richard Wertz et al.)

Table 16 Mission Mass Budget

Subsystem (% of Dry Mass)	Mass Budget (%)	Actual Mass (g)
Payload	41%	1200
Structure and Solar panel, Integrated sun sensors + gyroscope	20%	850 +390
battery	19%	0.125+ 0.125
TT&C	2%	1000
Attitude Determination and Control and On-Board Processing, orbit determination	8%+5%+2%	1700
Antenna	3%	40
Total	100%	5180.25

5. Discussion

5.1 Finding

This study aimed to assess the feasibility of deploying a constellation of CubeSats in Low Earth Orbit (LEO) to obtain daily sea level measurements in coastal areas focusing on the use of the GNSS-Reflectometry (GNSS-R) as an alternative to the traditional radar altimetry methods.

The study found that the GNSS-R receiver can be an alternative to conventional radar altimetry. The GNSS-R receiver offers an alternative, cost-effective approach to acquiring new data for sea level measurement by reducing the cost of instrumentation and weight. The receiver does not require a dedicated transmitter and uses an already available GNSS signal. This reduces the instrument's mass, power requirements and overall mission cost. However, it was found that the GNSS-R receiver still has challenges with signal processing, and further algorithm refinement is needed. To reduce the errors due to ionospheric delay, as they are still causing a systematic error

The primary mission requirement is to achieve accurate measurements near the coastal area and ensure continuous sea-level measurement. The study has analysed past and current missions by evaluating the key factors such as the mission requirements, constraints, budget, weight, and the need for high space and temporal data using the GNN-R platform.

The study selected an orbit that ensures continuous power for the GNSSR receiver, accessibility, and the desired spatial resolution. This orbit was also ideal for GNSSR missions, supported by successful missions such as the UK-DOT-1, FSSCat, FengYun-3E, and HydroGNSS. It was found that the FSSCat and Cat-3/MOTS GNSS-R missions deployed on sun-synchronous orbit (SSO), the orbit enabled the mission for global coverage and regional coverage (Castellví et al., 2018).

The analyses of CYGNSS GNSS-R constellations missions have shown their effectiveness in providing observation space-time remote sensing using satellites. The study found that using constellations between 4 and 8 satellites arranged in a Walker-Delta altimetric precision has improved from 0.3158m to 0.2231(Zhang et al. 2024). The eight satellites can be placed in one plane was shown to enhance the revisit time.

The Mission analysis for access and contact time has shown at least 10 minutes of contact and almost daily contact time. In addition, the data rate calculation was conducted based on the CYGNSS mission data per day; the result has shown that with the selected transceiver, we can transfer up to 405.3 MB of data per pass. This calculation shows promise as it exceeds the CYGNSS mission downlink data per day.

A satellite lifetime calculation was executed to analyse how long the satellite decays to an altitude of 180km. The results showed that the satellite takes almost 70 elapsed days to decay to 180 – 200 km altitude. This can be improved by selecting the right ground station and conducting further orbital simulations compared to the average CubeSat mission duration of two to five years.

The preliminary power consumption calculation was performed, and two solar panels can generate 36.8w for the whole satellite; this preliminary result shows that it can sustain the power consumption needed during the nominal operation. Power Systems (EPS) 30%, ADCS 15% ,Command & Data Handling System (CDHS)5%, On-Board Computer5%, Payload40%.

Overall, the study has shown high Spatial and temporal resolution requirements set at an accuracy of ~1-2 cm, and a revisit Period of 1-2 days can be achieved by using Walker-Delta constellations arranged between 4 and 8 of 6U CubeSats.

6. Conclusion

This study aimed to assess the feasibility of using CubeSat to monitor sea levels in coastal areas. It has been shown that CubeSats is a valuable tool for responding to the need for a high temporal observation frequency. Also, it can be an alternative, cost-effective way to monitor the sea level of the GNSS-R receiver. For this mission, it was found that the SSO orbit at around 550 km altitude and with 15 orbits per day can increase the special resolution.

This mission can achieve similar achievements of past missions such as CYGNSS, FSSCat, and FengYun-3E. The mission will benefit from technological advancements, such as artificial intelligence, to optimise data processing, similar to the FSSCat mission. Overall, this study has shown that the mission could be feasible.

7. Recommendations for Further Work

This study didn't cover the cost analyses due to time constraints. The study will benefit from further cost analyses.

8. References

- Abdalla, S. et al., 2021. Altimetry for the future: Building on 25 years of progress [online]. *Advances in Space Research*, 68(2), pp.319–363. Available at: <https://linkinghub.elsevier.com/retrieve/pii/S0273117721000594> [Accessed 8 June 2024].
- Abdullah, N.N. et al., 2018. Validation and Quality Assessment of Sea Levels from SARAL/ AltiKa Satellite Altimetry over the Marginal Seas at the Southeast Asia [online]. *Multi-purposeful Application of Geospatial Data*. Available at: <https://www.intechopen.com/chapters/59549> [Accessed 17 June 2024].
- Ablain, M. et al., 2017. Satellite Altimetry-Based Sea Level at Global and Regional Scales [online]. *Surveys in Geophysics*, 38(1), pp.7–31. Available at: <https://link-springer-com.nottingham.idm.oclc.org/article/10.1007/s10712-016-9389-8> [Accessed 10 June 2024].
- AC Clyde Space (2021). Space Products & Components | AAC Clyde Space. [online] AAC Clyde Space. Available at: <https://www.aac-clyde.space/what-we-do/space-products-components> [Accessed 28 Aug. 2024].
- Adebisi, N., Balogun, A.-L., et al., 2021. Advances in estimating Sea Level Rise: A review of tide gauge, satellite altimetry and spatial data science approaches [online]. *Ocean & Coastal Management*, 208, p.105632. Available at: <https://linkinghub.elsevier.com/retrieve/pii/S0964569121001174> [Accessed 7 April 2024].
- Adebisi, N., Balogun, A.L., et al., 2021. Advances in estimating Sea Level Rise: A review of tide gauge, satellite altimetry and spatial data science approaches. *Ocean & Coastal Management*, 208, p.105632. 10.1016/J.OCECOAMAN.2021.105632.
- Amani, M. et al., 2022a. Remote Sensing Systems for Ocean: A Review (Part 2: Active Systems). *IEEE Journal of Selected Topics in Applied Earth Observations and Remote Sensing*, 15, pp.1421–1453. 10.1109/JSTARS.2022.3141980.
- Amani, M. et al., 2022b. Remote Sensing Systems for Ocean: A Review (Part 2: Active Systems). *IEEE Journal of Selected Topics in Applied Earth Observations and Remote Sensing*, 15, pp.1421–1453. 10.1109/JSTARS.2022.3141980.
- An, C. et al., 2022. A review on the research progress of lake water volume estimation methods. *Journal of Environmental Management*, 314, p.115057. 10.1016/J.JENVMAN.2022.115057.
- Asharaf, S. et al., 2021. CYGNSS ocean surface wind validation in the tropics. *Journal of Atmospheric and Oceanic Technology*, 38(4), pp.711–724. 10.1175/JTECH-D-20-0079.1.
- Bašić, T., Bašić, T., 2023. Introductory Chapter: Satellite Altimetry – Overview [online]. *Satellite Altimetry - Theory, Applications and Recent Advances*. Available at: <https://www.intechopen.com/chapters/87727> [Accessed 10 June 2024].
- Burkhard, C., Weston, S., 2021. The Evolution of CubeSat Spacecraft Platforms [online]. *Conference Paper*. Available at: <https://www.nanosats.eu/> [Accessed 28 July 2022].
- Bussy-Virat, C.D., Ruf, C.S., Ridley, A.J., 2019. Relationship between Temporal and Spatial Resolution for a Constellation of GNSS-R Satellites. *IEEE Journal of Selected Topics in Applied Earth Observations and Remote Sensing*, 12(1), pp.16–25. 10.1109/JSTARS.2018.2833426.
- Castellví, J., Camps, A., Corbera, J. and Alamús, R. (2018). 3Cat-3/MOTS Nanosatellite Mission for Optical Multispectral and GNSS-R Earth Observation: Concept and Analysis. *Sensors*, 18(2), p.140. doi:<https://doi.org/10.3390/s18010140>.
- Cheong, J.W. et al., 2020. A Robust Framework for Low-Cost Cubesat Scientific Missions: In-Orbit Recovery, Results and Lessons Learned from UNSW-ECO [online]. *Space Science Reviews*, 216(1), pp.1–26. Available at: <https://link.springer.com/article/10.1007/s11214-019-0632-8> [Accessed 8 August 2022].

Helen Haile helen.haile1@nottingham.ac.uk

- Cipollini, P., Snaith, H., 2015. A short course on Altimetry [online]. *National Oceanography Centre, Southampton, U.K.* . Available at: https://eo4society.esa.int/wp-content/uploads/2021/02/2015Ocean_Cipollini_Altimetry1.pdf [Accessed 17 June 2024].
- Colagrossi, A. et al., 2023. Sensors. *Modern Spacecraft Guidance, Navigation, and Control: From System Modeling to AI and Innovative Applications*, pp.253–336. 10.1016/B978-0-323-90916-7.00006-8.
- Davis Dexter, Sutherland Michael, Sandesh JAGGAN, 2010. (PDF) Augmenting Tide Gauge Data with Satellite Altimetry in the Observation of Sea Level Rise in the Caribbean [online]. https://www.researchgate.net/publication/242602586_Augmenting_Tide_Gauge_Data_with_Satellite_Altimetry_in_the_Observation_of_Sea_Level_Rise_in_the_Caribbean, pp.2–6. Available at: https://www.researchgate.net/publication/242602586_Augmenting_Tide_Gauge_Data_with_Satellite_Altimetry_in_the_Observation_of_Sea_Level_Rise_in_the_Caribbean [Accessed 8 June 2024].
- Ecuadorian Civilian Space Agency (2007). EXA- ECUADORIAN SPACE AGENCY. [online] Exa.ec. Available at: <http://exa.ec/index-en.html?ref=satcatalog.com> [Accessed 30 Aug. 2024].
- Endurasat (2024). 6U Solar Panel - EnduroSat. [online] EnduroSat. Available at: <https://www.endurosat.com/products/6u-solar-panel/> [Accessed 18 Jul. 2024].
- Fasullo, J.T., Gent, P.R., Nerem, R.S., 2020. Forced Patterns of Sea Level Rise in the Community Earth System Model Large Ensemble From 1920 to 2100 [online]. *Journal of Geophysical Research: Oceans*, 125(6), p.e2019JC016030. Available at: <https://onlinelibrary.wiley.com/doi/full/10.1029/2019JC016030> [Accessed 6 June 2024].
- Fu, L.L. et al., 2024. The Surface Water and Ocean Topography Mission: A Breakthrough in Radar Remote Sensing of the Ocean and Land Surface Water [online]. *Geophysical Research Letters*, 51(4), p.e2023GL107652. Available at: <https://onlinelibrary.wiley.com/doi/full/10.1029/2023GL107652> [Accessed 29 June 2024].
- Gao, F. et al., 2018. Spatiotemporal Evaluation of GNSS-R Based on Future Fully Operational Global Multi-GNSS and Eight-LEO Constellations [online]. *Remote Sensing 2018, Vol. 10, Page 67*, 10(1), p.67. Available at: <https://www.mdpi.com/2072-4292/10/1/67/htm> [Accessed 3 July 2024].
- Garola, A., López-Dóriga, U., Jiménez, J.A., 2022. The economic impact of sea level rise-induced decrease in the carrying capacity of Catalan beaches (NW Mediterranean, Spain). *Ocean & Coastal Management*, 218, p.106034. 10.1016/J.OCECOAMAN.2022.106034.
- Gower, J., Barale, V., 2024. The Rising Concern for Sea Level Rise: Altimeter Record and Geo-Engineering Debate [online]. *Remote Sensing 2024, Vol. 16, Page 262*, 16(2), p.262. Available at: <https://www.mdpi.com/2072-4292/16/2/262/htm> [Accessed 29 June 2024].
- Grgić, M. et al., 2021. Radar Satellite Altimetry in Geodesy - Theory, Applications and Recent Developments [online]. *Geodetic Sciences - Theory, Applications and Recent Developments*. Available at: <https://www.intechopen.com/chapters/76245> [Accessed 17 June 2024].
- Hamid, A.I.A. et al., 2018. Contemporary sea level rise rates around Malaysia: Altimeter data optimization for assessing coastal impact. *Journal of Asian Earth Sciences*, 166, pp.247–259. 10.1016/J.JSEAES.2018.07.034.
- Han, S. et al., 2014. Minimum of PDOP and its applications in inter-satellite links (ISL) establishment of Walker- δ constellation. *Advances in Space Research*, 54(4), pp.726–733. 10.1016/j.asr.2014.04.020.
- Han, Y., Luo, J. and Xu, X. (2019). On the Constellation Design of Multi-GNSS Reflectometry Mission Using the Particle Swarm Optimization Algorithm. *Atmosphere*, [online] 10(12), pp.807–807. doi:<https://doi.org/10.3390/atmos10120807>.
- Hannah, John, 2010. The Problems and Challenges in Using Tide Gauges to Monitor Long-term sea Level Change [online]. *FIG Peer Review Journal*. Available at: <https://www.fig.net/resources/publications/prj/showpeerreviewpaper.asp?pubid=3786> [Accessed 29 June 2024].

Helen Haile helen.haile1@nottingham.ac.uk

- Honeywell (2024). Telemetry, Tracking & Command (TT&C) Products. [online] aerospace.honeywell.com. Available at: <https://aerospace.honeywell.com/us/en/products-and-services/product/hardware-and-systems/space/small-satellite-specific-bus-products/telemetry-tracking-command> [Accessed 29 Aug. 2024].
- James Richard Wertz, et al. Space Mission Engineering : The New SMAD. Torrance, Microcosm Press, 2011.
- Japan Association of Remote Sensing (1996). 2.1 Types of Sensor. [online] sar.kangwon.ac.kr. Available at: http://sar.kangwon.ac.kr/etc/rs_note/rsnote/cp2/cp2-1.htm [Accessed 26 Aug. 2024].
- Jiang, X., Jia, Y., Zhang, Y., 2019. Measurement analyses and evaluations of sea-level heights using the HY-2A satellite's radar altimeter [online]. *Acta Oceanologica Sinica*, 38(11), pp.134–139. Available at: <https://link.springer.com/article/10.1007/s13131-019-1503-6> [Accessed 24 June 2024].
- Jin, S. et al., 2024. Remote sensing and its applications using GNSS reflected signals: advances and prospects [online]. *Satellite Navigation 2024 5:1*, 5(1), pp.1–42. Available at: <https://satellite-navigation.springeropen.com/articles/10.1186/s43020-024-00139-4> [Accessed 15 July 2024].
- Leyva-Mayorga, I., Soret, B., Matthiesen, B., Röper, M., Wübben, D., Dekorsy, A. and Popovski, P. (2022). NGSO Constellation Design for Global Connectivity. arXiv:2203.16597 [cs, eess]. [online] doi:<https://doi.org/10.1049/PBTE105E>.
- L. Sánchez, D. Chambers, K.H., 2024. Sea Surface Heights [online]. Available at: <https://ggos.org/item/sea-surface-heights/#learn-this> [Accessed 12 June 2024].
- LI, W. et al., 2021. First spaceborne demonstration of BeiDou-3 signals for GNSS reflectometry from CYGNSS constellation. *Chinese Journal of Aeronautics*, 34(9), pp.1–10. 10.1016/J.CJA.2020.11.016.
- Liu, Z. et al., 2021. Relationship Between Altimetric Quality and Along-Track Spatial Resolution for iGNSS-R Sea Surface Altimetry: Example for the Airborne Experiment [online]. *Frontiers in Earth Science*, 9, p.730513. Available at: www.frontiersin.org [Accessed 24 July 2024].
- Loff, S., 2018. CubeSats Overview | NASA [online]. Available at: https://www.nasa.gov/mission_pages/cubesats/overview [Accessed 29 July 2022].
- Ma, D.M., Zhai, S.Y., 2004. Sun-synchronous satellite orbit determination. *Acta Astronautica*, 54(4), pp.245–251. 10.1016/S0094-5765(03)00031-6.
- Marcos, M. et al., 2019. Coastal Sea Level and Related Fields from Existing Observing Systems [online]. *Surveys in Geophysics 2019 40:6*, 40(6), pp.1293–1317. Available at: <https://link.springer.com/article/10.1007/s10712-019-09513-3> [Accessed 8 June 2024].
- Markus, T. et al., 2017. The Ice, Cloud, and land Elevation Satellite-2 (ICESat-2): Science requirements, concept, and implementation. *Remote Sensing of Environment*, 190, pp.260–273. 10.1016/J.RSE.2016.12.029.
- McMillan, M. et al., 2018. Assessment of CryoSat-2 interferometric and non-interferometric SAR altimetry over ice sheets. *Advances in Space Research*, 62(6), pp.1281–1291. 10.1016/J.ASR.2017.11.036.
- McClaren, A. (2023). The State of GNSS Receiver Tracking Channels & Satellite Constellations in Orbit. [online] geospatial.trimble.com. Available at: <https://geospatial.trimble.com/en/resources/blog/gnss-receiver-channels-and-satellite-tracking> [Accessed 28 Jul. 2024].
- Quartly, G., Chen, G., 2006a. Introduction to the Special Issue on 'Satellite Altimetry: New Sensors and New Applications' [online]. *Sensors 2006, Vol. 6, Pages 616–619*, 6(6), pp.616–619. Available at: <https://www.mdpi.com/1424-8220/6/6/616/htm> [Accessed 19 June 2024].
- Quartly, G., Chen, G., 2006b. Introduction to the Special Issue on 'Satellite Altimetry: New Sensors and New Applications' [online]. *Sensors 2006, Vol. 6, Pages 616–619*, 6(6), pp.616–619. Available at: <https://www.mdpi.com/1424-8220/6/6/616/htm> [Accessed 22 July 2024].

Helen Haile helen.haile1@nottingham.ac.uk

- Quartly, G.D., Rinne, E., Passaro, M., Andersen, O., Dinardo, S., Fleury, S., Guerreiro, K., Guillot, A., Hendricks, S., Kurekin, A.A., Müller, F.L., Ricker, R., Skourup, H. and Tsamados, M. (2018). Review of Radar Altimetry Techniques over the Arctic Ocean: Recent Progress and Future Opportunities for Sea Level and Sea Ice Research. Biogeosciences (European Geosciences Union). doi:<https://doi.org/10.5194/tc-2018-148>.
- Rodriguez-Alvarez, N., Munoz-Martin, J.F., Morris, M., 2023. Latest Advances in the Global Navigation Satellite System—Reflectometry (GNSS-R) Field [online]. *Remote Sensing* 2023, Vol. 15, Page 2157, 15(8), p.2157. Available at: <https://www.mdpi.com/2072-4292/15/8/2157/htm> [Accessed 2 July 2024].
- Roy, P. et al., 2023. Effects of climate change and sea-level rise on coastal habitat: Vulnerability assessment, adaptation strategies and policy recommendations. *Journal of Environmental Management*, 330, p.117187. 10.1016/J.JENVMAN.2022.117187.
- Ruf, C.S., Gleason, S., Zorana Jelenak, Katzberg, S.J., Ridley, A.J., Rose, R.L., Scherrer, J. and Zavorotny, V.U. (2012). The CYGNSS nanosatellite constellation hurricane mission. IEEE International Geoscience and Remote Sensing Symposium. doi:<https://doi.org/10.1109/igarss.2012.6351600>.
- Sánchez, D, L. and Chambers, D. (2024). Sea Surface Heights. [online] GGOS. Available at: <https://ggos.org/item/sea-surface-heights/#toggle-id-1>.
- Tyvak. "LAUNCH of FSSCAT and OSM-1 - Tyvak." Tyvak, 2 Sept. 2020, tyvak.eu/launch-of-fsscat-and-osm-1/. Accessed 1 Sept. 2024.
- US Department of Commerce, N.O. and A.A. (n.d.). How are Tides Measured? - The New System - Tides and Water Levels: NOAA's National Ocean Service Education. [online] oceanservice.noaa.gov. Available at: https://oceanservice.noaa.gov/education/tutorial_tides/tides11_newmeasure.html [Accessed 28 Aug. 2024].
- Venturini, C.C., 2017. Improving Mission Success of CubeSats.
- Villela, T. et al., 2019. Towards the thousandth CubeSat: A statistical overview [online]. *International Journal of Aerospace Engineering*, 2019. Available at: <https://www.hindawi.com/journals/ijae/2019/5063145/> [Accessed 6 August 2022].
- Xing, J. et al., 2022. A Real-Time GNSS-R System for Monitoring Sea Surface Wind Speed and Significant Wave Height [online]. *Sensors* 2022, Vol. 22, Page 3795, 22(10), p.3795. Available at: <https://www.mdpi.com/1424-8220/22/10/3795/htm> [Accessed 3 July 2024].
- Xu, T. et al., 2024. GNSS Reflectometry-Based Ocean Altimetry: State of the Art and Future Trends [online]. *Remote Sensing* 2024, Vol. 16, Page 1754, 16(10), p.1754. Available at: <https://www.mdpi.com/2072-4292/16/10/1754/htm> [Accessed 8 July 2024].
- youmatter.world (2019). Sea Level Rise Definition. [online] youmatter-. Available at: <https://youmatter.world/en/definitions/sea-level-rise-definition/> [Accessed 30 Jul. 2024].
- Zhang, Y., Zheng, W., Liu, Z., 2024. Improving the spaceborne GNSS-R altimetric precision based on the novel multilayer feedforward neural network weighted joint prediction model. *Defence Technology*, 32, pp.271–284. 10.1016/J.DT.2023.03.019.

8. Appendices

Appendix A: Project Plan

Dissertation Timeline		March				April				May				June				July				August			
Task No.	Description	W1	W2	W3	W4	W1	W2	W3	W4	W1	W2	W3	W4	W1	W2	W3	W4	W1	W2	W3	W4	W1	W2	W3	W4
1	Topic finding																								
1.1	Read through lecture notes and assignments for topic inspiration																								
1.2	Background Reading																								
1.3	Select and start learning to use reference management software																								
1.4	Preliminary research:																								
1.5	Refine topic into research questions																								
1.6	Write preliminary objectives for achieving my research question																								
1.7	Draft Proposal																								
1.8	Amend topic focus/ plan based on supervisor feedback																								
2	Proposal																								
2.1	Write up agreed research question and objectives																								
2.2	Research methodologies																								
2.3	Create bibliography and reference list																								
2.4	Edit																								
2.5	Submit proposal																								
2.6	Poster Drafting																								
2.7	Edit submit poster																								
3	Literature review																								
3.1	Refresh searching skills (attend workshop or complete online)																								
3.2	Read through materials gathered																								
3.3	Introduction/ Aim & Objectives Chapters																								
3.4	Proof reading introduction																								
3.5	Data management																								
3.6	Literature Review Chapter																								
3.7	Interim report																								
3	Methodology																								
3.1	Select and prepare methods																								
3.2	Critique methodology																								
3.3	Meet supervisor																								
3.4	Update bibliography and write up methodologies section																								
4	Data collection and analysis																								
4.1	Review results and methodology																								
4.2	Record results and evaluate Results																								
4.3	Write up data analysis section																								
5	Writing																								
5.1	Write up remaining sections																								
5.2	Review and improve writing																								
5.3	Proofread																								
5.4	Add charts, displays to data analysis sections.																								
5.5	Bibliography, Figures & Tables																								
6	finishing off																								
6.1	Final proof read and re-writing																								
6.2	Poster																								
6.3	Submit																								
	Legends																								
	Topic finding																								
	Proposal																								
	Literature review																								
	Methodology																								
	Data collection and analysis																								
	Writing																								
	finishing off and submissions																								

Appendix B: Orbital calculation

Table B1 Orbital Calculation 1

Parameter	Unit	Equation	Input
Orbital period (T)	Second	$T = \sqrt{\frac{4\pi^2 R^3}{\mu_E}}$ $T = \sqrt{\frac{(4\pi^2 \times 6921^3)}{3.986 \times 10^5}}$ $= 5777.430s \sim 96.26 \text{ min}$	Altitude =550 km. $\mu_E : 3.986 \times 10^5 \text{ (Km}^3 \text{ /s}^2 \text{)}$ Re: Earth's radius 6378(km) h: orbital altitude (km)
Number of orbits per day	Second	$\frac{1h = 3600s}{5777.430s} = 1h60s$ $1 \text{ day} = 24h = 3600 \frac{s}{h} \times 24h = 86400s$ $CapNumber \text{ of orbits per day} = \frac{86400s}{5777.43s} = 14.9547$ $\approx 15 \text{ orbits per day}$	
Earth's angular Radius (ρ)	Degrees	$\rho = \sin^{-1} (R/h+R)$ $\sin^{-1} (6378 / 550+6378)$ $= 67.015718120449$	ρ : Earther angular radius
Time of Eclipse (TE)	Second	$TE = (2\rho / 360^\circ) * T = 2150.807s$	Orbital period (T)
Time in sunlight (TS)	Second	$TS = T - TE$ $TS = 5777.430s - (2150.80[s]) TS = 3626.63s$	Time Of eclipse (TE)
Semi Major Axis (a)		$a = R_E + h = 6371 \text{ km} + 550 \text{ km} = 6,921 \text{ km}$	$R_E = 6371 \text{ km}$ $h = 550 \text{ km}$
Inclination (i)		The sun-synchronous orbit (SSO) has around $i = 97.57 \sim 98^\circ$	
Eccentricity (e)		$e = \frac{c}{a}$	e eccentricity is equal to zero for a circular orbit
True anomaly(v)		$\theta = \tan^{-1} \left(\frac{\sqrt{1-e^2} \sin(E)}{\cos(E)-e} \right) \quad \theta = \tan^{-1} \left(\frac{\sqrt{1-e^2} \sin(E)}{\cos(E)-e} \right)$	
Mean anomaly	Degree	$M = \frac{2\pi}{P} (\Delta t) + M_0$	satellite without orbital changes, the mean anomaly, M, is computed using the uniform equation of motion in terms of the orbital period P and the mean anomaly at the initial epoch
Argument of Perigee (ω)	Degree	The argument of perigee is the angle between the ascending node and the periapsis point of the orbit. $\frac{d\omega}{dt} = \frac{3nJ_2 R_E^2 (4-5\sin^2 i)}{4a^2 (1-e^2)^2}$	When $i = 0$ or 180° (equatorial orbit) or $e = 0$ (circular orbit)
Right Ascension of Ascending Node (Ω)	Degree	$\dot{\Omega} = -3/2 J_2 \mu R^2 a^{-7/2} \cos i$ <p>For a sun-synchronous orbit (SSO), the precession rate matches the Sun direction motion (0.986 deg/day)</p>	$R_T = 6378137m$ $\mu = 3.986005.1014m^3/s^2$ $J_2 = 1.08266$
Mean motion	(rev/day)	$a = \left(\left(\frac{P}{2\pi} \right)^2 \mu \right)^{\frac{1}{3}} \sim a = \left(\left(\frac{5777.430}{2\pi} \right)^2 * 3.986 \times 10^5 \right)^{\frac{1}{3}}$ $a = 6959.034 \frac{rev}{day}$	
local elevation angle (El)	Degree	$El = \cos^{-1} \left(\frac{Rt}{d} \sin \gamma \right)$	$D = \text{slant path}$ $Rr = \text{radial distance}$

radial distance (r)		$r = \frac{a(1-e^2)}{1+ecos(\theta)} \sim r = \frac{a(1-e^2)}{1+ecos(\theta)}$	radial distance (r) the radial distance from the centre of the earth to each spacecraft in the simulation using
Ponting angle Φ	Degree	$\Phi = 90^\circ - \text{El}$ 85	5 degrees from the ground station
Orbital velocity	Km/s	$V = \sqrt{\frac{\mu_E}{a}} \quad V = \sqrt{\frac{3.986 \times 10^{14} \frac{m^3}{s^2}}{6,921 \times 10^3 m}}$ $= 7588.99 \frac{m}{s} = 7.589 \frac{km}{s}$	μ_E – Earth's standard gravitational parameter = $3.986 \times 10^{14} \text{ m}^3/\text{s}^2$
Specific orbital energy (ϵ)		$\epsilon = -\frac{\mu_E}{2a}$ $\epsilon = -\frac{3.986 \times 10^{14} \frac{m^3}{s^2}}{2 \times 6,921 \times 10^3 m} = -28796416.70$ $-28.8 \frac{MJ}{kg}$	Altitude = 550 km. $\mu_E : 3.986 \times 10^5 \text{ (Km}^3 \text{ /s}^2 \text{)}$ Re = 6378(km) a = 6,921 km

Appendix C: Constellations Calculation**Input**

- **Semi-major Axis (a):** 6,921 km
- **Eccentricity (e):** 0 (circular orbit)
- **Inclination (i):** 98°
- **Earth's Rotation Rate (ω_E):** 2π radians/day
- **Number of Orbits per Day (D):** 15
- **Orbital Period (T):** 5,777.430 s (or about 96.26 minutes)
- **Number of orbital planes (N):** 1 -2

Steps to Calculate RAAN Change Rate ($\dot{\Omega}$)

By using the formula

$$D \cdot 2\pi \cdot \omega_E - \dot{\Omega} = N \cdot 2\pi \cdot M + \omega$$

Calculate Mean Motion (M): $M = \frac{2\pi}{T}$ $M = \frac{2\pi}{5777.430}$ $M \sim 1.085 \times 10^{-3} \text{ rad/s}$

Converting the orbital period T into seconds and days :

$$T_{\text{days}} = \frac{T}{86400} = \frac{5777.430\text{s}}{86400\text{s}} = 0.0669 \text{ days}$$

Right Ascension of the Ascending Node:

Earth's rotation rate = $\frac{2\pi \text{ radians}}{\text{day}} = 2 \frac{\pi}{86400\text{s}} = 7.272 \times 10^{-5} \text{ rad/s}$

Number of orbital planes (N): 1 -2

By using the formula

$$D \cdot 2\pi \cdot \omega_E - \dot{\Omega} = N \cdot 2\pi \cdot M + \omega$$

$$\dot{\Omega} = D \cdot \omega_E - N \cdot M$$

$$\dot{\Omega} = 15 \cdot 7.272 \times 10^{-5} - 1 \cdot 1.085 \times 10^{-3} \text{ rad/s}$$

$$\dot{\Omega} = 6 \times 10^{-6} \text{ rad/s}$$

Calculation for two orbital planes

$$\dot{\Omega} = 15 \cdot 7.272 \times 10^{-5} - 2 \cdot 1.085 \times 10^{-3} \text{ rad/s}$$

$$\dot{\Omega} = -1.0792 \times 10^{-3} \text{ rad/s}$$

The constellations must be in one plane as the RAAN change plane is negative with 2 planes. Therefore, for this mission, only one plane will be considered.

$$\text{spacing} = \frac{360^\circ}{\text{number of satellites per plane}}$$

$$\text{spacing} = \frac{360^\circ}{58} = 45^\circ$$

Coverage Analysis: To determine the reflecting ground coverage for the GNSS-R off-nadir antenna by using preliminary input from the CYGNSS mission

1. Beamwidth Calculation

Beamwidth of the Antenna: $14.5 \text{ dBic} \times 2$

Panels off point 28°

Rearranging the formula to calculate the neglecting the frequency wavelength

$$BM = 70 \times WLD$$

$$BM = 70 \text{ Gain in dBic}$$

$$BM = 70 / 14.5 = 4.83 \text{ degree}$$

2. Footprint Radius calculation:

Estimated based on antenna beamwidth and altitude

ϵ is the elevation angle of the ground station antenna = 5°

Beamwidth θ : 4.83 degree

$R_e = 6371 \text{ km}$

$$\theta = 4.83 \times \frac{\pi}{180} \sim 0.0843 \text{ radians}$$

Calculate Angular Radius:

$$\theta = \cos^{-1}\left(\frac{R_e}{R_e + h}\right)$$

$$\cos^{-1}\left(\frac{6371}{6371 + 550}\right) = 22.99 \sim 23 \sim 0.401 \text{ - in radian}$$

To calculate the foot radius

$$R = R_e \theta$$

$$R_e = 6371 \times 0.0843 = 537.5 \text{ km}$$

3. Coverage Area: by using the Coverage of the satellite

$R = 40589641 \text{ km}^2$

$$S = 2\pi R_e^2 (1 - \cos\theta)$$

$$S = 2\pi 6371^2 (1 - \cos 0.0843)$$

$$S = 2\pi 6371^2 (0.01)$$

$$S = 865000 \text{ km}^2$$

Percentage Coverage Calculation $A \% = 1/2 (1 - \cos\beta)$

Appendix D: Power calculation

Table D1 Power Budget calculation 1

Aspect/Units	Value (s)	Value (h)	Calculation (1 Solar Panel)	Calculation (2 Solar Panels)	EnduraSat Solar Panel (1 Panel)	EnduraSat Solar Panel (2 Panels)
Orbital Period (T)/s	5063.22	1.4064				
Earth's Angular Radius (ρ)/degrees	67.01	67.01				
Time of Eclipse (TE)/s	1884.92	0.5235				
Time in Sunlight (TS)/s	3178.3	0.88				
Energy Required During Eclipse (EE)/Wh	0.7721	0.7721				
Energy Required During Sunlight (ES)/Wh	1.514	1.514				
Total Energy Required Per Orbit/Wh	2.2861	2.2861				
Solar Array Power Required (PSAR)/W			2.589	2.589	2.589	2.589
Power Generated at BOL/W			18.33	36.66	19.2	38.4
Power Generated at EOL/W			5.174	10.34	5.574 (29% efficiency)	11.148 (29% efficiency)
Power Efficiency at EOL/%			28.20%	28.20%	29%	29%
Solar Array Power Margin at BOL/W			18.33 W - 2.589 W = 15.741 W	36.66 W - 2.589 W = 34.071 W	19.2 W - 2.589 W = 16.611 W	38.4 W - 2.589 W = 35.811 W
Solar Array Power Margin at EOL/W			5.174 W - 2.589 W = 2.585 W	10.34 W - 2.589 W = 7.751 W	5.574 W - 2.589 W = 2.985 W	11.148 W - 2.589 W = 8.559 W
Battery Capacity (Batt)/Wh/	Energy Required During Eclipse (EE)/1-DOD	1.103				
DOD: 30% or 0.3						
Power Margin Analysis:						

Appendix E Payload Description

Table E1 Payload Description 1

Payload systems Preliminary subsystem Required	Description
Antennas	<p>Zenith antenna The GNSS directly reflects the signal received by the Zenith antenna. It is a dual-frequency (L1 and L2) right-hand circularly polarised (RHCP) antenna.</p> <p>Nadir antenna: It receives the reflected/scattered signals from GNSS satellites. It is a high-gain dual-frequency left-hand circularly polarised (LHCP)</p>
The low noise amplifier (LNA)	It enhances the signal-to-noise ratio (SNR) power
Navigation Unit	GNSS navigation unit provides position, velocity, and timing information.
RF front ends (RFFEs)	The RFFEs convert the incoming signal from analogue to digital.
Science Unit	The Unit is responsible for receiving and processing the GNSS signals.